eprints@whiterose.ac.uk
https://eprints.whiterose.ac.uk/

Alkali metal CO_2 sorbents and the resulting metal carbonates: Potential for process intensification of Sorption-Enhanced Steam Reforming

Muhammad Zaki Memon[†], Xiao Zhao[†], Vineet Singh Sikarwar[†], Arun K. Vuppaladadiyam[†], Steven J. Milne[‡], Andy P. Brown[‡], Jinhui Li[†] and Ming Zhao[†, §, ∥,*]

† School of Environment, Tsinghua University, Beijing, 100084, China

‡ School of Chemical and Process Engineering (SCAPE), University of Leeds, Leeds LS2 9JT, United Kingdom

§ Key Laboratory for Solid Waste Management and Environment Safety, Ministry of Education, Beijing, 100084, China

∥ Collaborative Innovation Center for Regional Environmental Quality, Tsinghua University, China

* Corresponding author. Tel/Fax: +86 10 6278 4701, Email: ming.zhao@tsinghua.edu.cn

ABSTRACT: Sorption-enhanced steam reforming (SESR) is an energy and cost efficient approach to produce hydrogen with high purity. SESR makes it economically feasible to use a wide range of feedstocks for hydrogen production such as methane, ethanol and biomass. Selection of catalysts and sorbents plays a vital role in SESR. This article reviews the recent research aimed at process intensification by the integration of catalysis and chemisorption functions into a single material. Alkali metal ceramic powders, including Li_2ZrO_3, Li_4SiO_4 and Na_2ZrO_3 display characteristics suitable for capturing CO_2 at low concentrations (< 15% CO_2) and high temperatures (> 500 °C), and thus are applicable to pre-combustion technologies such as SESR, as well as post-combustion capture of CO_2 from flue gases. This paper reviews the progress made in improving the operational performance of alkali metal ceramics under conditions that simulate power plant and SESR operation, by adopting new methods of sorbent synthesis and doping with additional elements. The paper also discusses the role of carbonates formed after in-situ CO_2 chemisorption during a steam reforming process in respect of catalysts for tar cracking.

TOC

Sorption Enhanced Steam Reforming

SP=Secondary phase   *MC= Metal Carbonate

Alkali Metal Sorbent (AMS)   *M = Li, Na

CO_2 release

CO_2 sorption

H_2

Hydrocarbons Cracking & Reforming

CO_2 sorption

SP MC MC SP SP MC

AMS SP MC AMS MC SP SP MC AMS

1. INTRODUCTION

Sorption-enhanced steam reforming (SESR) is a promising thermochemical approach to producing hydrogen-rich fuel gases, utilizing steam as a gasifying agent, and is applicable to multiple types of hydrocarbon feedstocks i.e. methane, ethanol and biomass to generate hydrogen.[1, 2] Hydrogen is a green energy carrier with a calorific value (of 122 kJ g^{-1}), that is greater than other hydrocarbon fuels.[3] SESR is a modification of the conventional steam reforming method of hydrogen production, and involves less intensive operating conditions than conventional steam methane reforming (SMR). In conventional SMR, methane is reformed in the presence of a catalyst and steam to produce syngas. The SMR process involves the following major reactions to produce hydrogen (Eqns. 1-3):

$$CH_4(g) + H_2O(g) \rightleftharpoons CO(g) + 3H_2(g), \qquad \Delta H_{298} = 206 \text{ kJ mol}^{-1} \qquad (1)$$

$$CH_4(g) + 2H_2O(g) \rightleftharpoons CO_2(g) + 4H_2(g), \qquad \Delta H_{298} = 164.5 \text{ kJ mol}^{-1} \qquad (2)$$

$$CO(g) + H_2O(g) \rightleftharpoons CO_2(g) + H_2(g), \qquad \Delta H_{298} = -41 \text{ kJ mol}^{-1} \qquad (3)$$
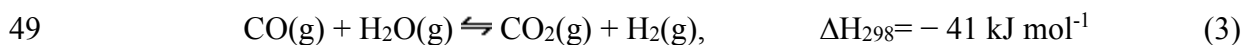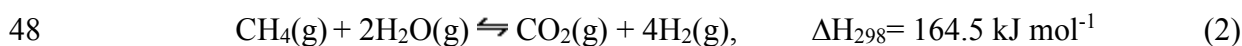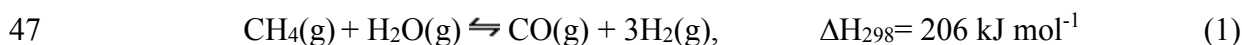
The conventional SMR process requires two separate chambers for these reactions because the endothermic methane reforming reactions, i.e. Eqns. (1) and (2), occur at high temperatures (> 800 °C) and low pressures, while the exothermic water-gas shift (WGS) reaction, Eqn. (3), occurs at lower temperatures (< 400 °C).[4] Additionally, the

54   hydrogen stream has to be separated from CO_2 during the WGS reaction. By introducing

55   a sorbent to capture CO_2 generated *in-situ* of the reforming reactions, the thermodynamic

56   limits placed on the process are less restrictive (**Figure 1**). Thereby methane reforming,

57   WGS and CO_2 removal (an exothermic reaction) can occur simultaneously in a single

58   chamber.[5] As such, SESR can be coupled with SMR to streamline a widely utilized

59   industrial procedure for hydrogen production. At the same time, SESR also provides an

60   opportunity to generate hydrogen from biomass feedstock; SESR is reported to produce

61   H_2 with purity > 85%, almost doubling the amount of hydrogen reported from previous

62   reactions.[1, 6, 7]
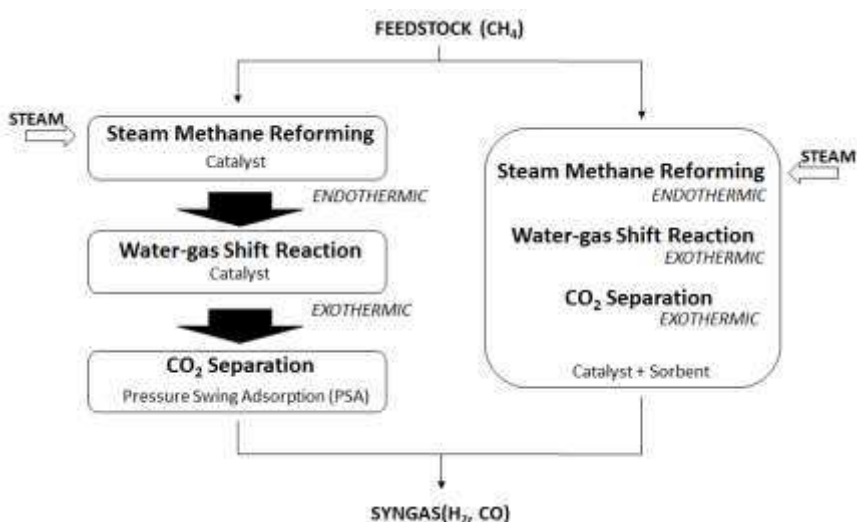
63

64   **Figure 1**. Simple schematic representations of SMR process (right) and SESR (left)

65   utilizing methane to produce H_2 enriched syngas.

66

67   The two vital materials that facilitate SESR are catalysts and sorbents. An appropriate

68   catalyst for biomass-fueled SESR must be capable of catalyzing both tar-cracking and

69   hydrocarbon reforming. Among the commonly used catalysts, Ni is widely regarded as

70   the most cost effective.[8] Nano-sized Ni particles can be widely dispersed on supports,

71   leading to increased catalytic activity. For the purpose of *in-situ* CO_2 capture, a sorbent

72   must possess selectivity towards CO_2 in a stream of mixed gases, an ability to confine

73   and release CO_2 within itself at high temperatures (400 °C and above), and capacity to

74   maintain mechanical integrity under duress of cyclic CO_2 capture-and-release process.

75   Solid CO_2 sorbents have been proven to be the appropriate choice for high-temperature

76   SESR (>400 °C),[9] and they have been widely researched for the removal of CO_2 from

77   flue gases.[9-11] This is an additional advantage of SESR because sequestration by the

78   sorbent can prevent CO_2 generated in-situ from being released into the atmosphere,

79   making the process net carbon negative when a carbon-neutral biomass is used as the

80   feedstock. Sorbents based on CaO are foremost among the solid sorbents that couple to

81   the reaction conditions of SESR.[12, 13] These sorbents are cheap and show promising

82   chemisorption capacity and kinetics, 17.8 mmol-CO_2 g-sorbent^{-1}, at the moderate-to-high

83   temperatures required for SESR (450-750 °C), however a drawback lies in the tendency

84   of CaO to sinter during regeneration (up to 900 °C), resulting in gradual deactivation over

85   a multicycle process. Hydrotalcites (HTlcs) trap CO_2 in the temperature range of 200-500

86   °C and exhibit improved performance under steam saturated atmospheres, despite HTlcs

87   being limited by poor chemisorption capacity, < 1.0 mmol-CO_2 g-sorbent^{-1}, and slow

88   reaction kinetics.[14] Magnesia, MgO is a naturally abundant resource, and active in

89   capturing CO_2 at low-to-moderate temperatures, i.e. 300-450 °C, have a CO_2

90   chemisorption capacity of < 3.4 mmol-CO_2 g-sorbent^{-1}, can be regenerated at 500 °C and

91   exhibits a positive influence of steam on its performance. But similar to CaO, MgO

92   sorbents deteriorate in a multi-cycle operation such as SESR.[15] An ideal sorbent should

93 retain its performance over multiple operating cycles. In the past decade, a great deal of

94 effort has been devoted to improve the sintering-resistance of these sorbents.[16, 17]

95   A recent research hotspot for SESR has been the development of a bifunctional

96 material (hybrid type) containing both active catalytic sites and chemisorption sites. The

97 most significant benefit of a bifunctional catalyst-sorbent is cost reduction as separate

98 catalyst and sorbent powders will no longer be needed. Theoretical studies conclude that

99 having catalyst and chemisorption sites closer will improve mass transfer as well as,

100 potentially maintain a relatively higher CO_2 partial pressure for chemisorption.[18] In

101 principle, CO_2 molecules would have shorter distance to travel to chemisorption sites at

102 or beneath the surface of the sorbent, resulting in faster reaction kinetics and lower

103 residence times in the reactor.[19]

104   Alkali metal ceramics, which in the context of this review refers to binary-metal

105 oxides composed of at least a metal belonging to the alkali metal group of chemical

106 elements, have been widely researched as alternative sorbents to CaO, due to their ability

107 to trap CO_2 as alkali metal carbonates under a wide range of temperatures. [20] Examples

108 include Li_2ZrO_3, Li_4SiO_4 and Na_2ZrO_3. The carbonates can be decomposed at higher

109 temperatures making the materials suitable for multi-cycle operations that involve CO_2

110 capture and release, i.e. both post- and pre-combustion capture schemes. Furthermore,

111 alkali metal ceramics offer useful catalytic activity for steam reforming processes. Alkali

112 metal zirconates such as Na_2ZrO_3 are reported to be active in catalyzing CO conversion

113 to CO_2; [21] and, their carbonated derivatives, i.e. Na_2CO_3 and K_2CO_3, formed after CO_2 is

114 chemisorbed, are common mineral components in biomass and have been investigated for

115 tar removal applications during biomass gasification.[8, 22, 23] Alkali metal carbonates have

116 also been reported as catalysts in methane reforming, the WGS reaction,[8] and

117 transesterification of soybean oil.[24] Therefore, alkali metal ceramics have potential to act

118 as a bifunctional catalyst-sorbent for SESR, even without grafting additional catalyzing

119 sites (such as inclusion of Ni nanoparticles).

120 After a brief review of a variety of recently developed bifunctional hybrid materials,

121 this article discusses in detail the potential of alkali metal ceramics as a standalone

122 bifunctional material in SESR, particularly with respect to the most widely researched

123 alkali-based sorbents Li_2ZrO_3, Li_4SiO_4 and Na_2ZrO_3. Modelling studies have suggested

124 these sorbents can be capable of producing up to 95 vol. % H_2 in SESR of methane and

125 ethanol and as such are discussed in this review. [25-28] Research into the catalytic role of

126 alkali metal ceramics in SESR is also summarized. Finally, investigations of synthesis

127 methods, means of modifying the performance of the materials and the effects on CO_2

128 chemisorption are discussed.

129 **2. BIFUNCTIONAL CATALYST-SORBENT HYBRID MATERIALS**

130 Given the advantages of incorporating the WGS reaction and product stream

131 purification in a single chamber it is not surprising that the use of CO_2 sorbents (SESR)

132 have attracted so much recent interest.[6, 29] Catalysts and sorbents need however to be

133 mixed before inserting in the reactor because it is extremely challenging to achieve

134 uniform mixing and avoid chemical inter-diffusion and loss of activity during operation.

135 As SESR produces a high-purity stream of hydrogen following Le Chatelier's principle,

136 any delay in removal of the product gas CO_2 is detrimental to the production of hydrogen.

137 A more direct removal of CO_2 is possible if catalyst and sorbent sites are intermixed in a

138 single material (**Figure 2**).
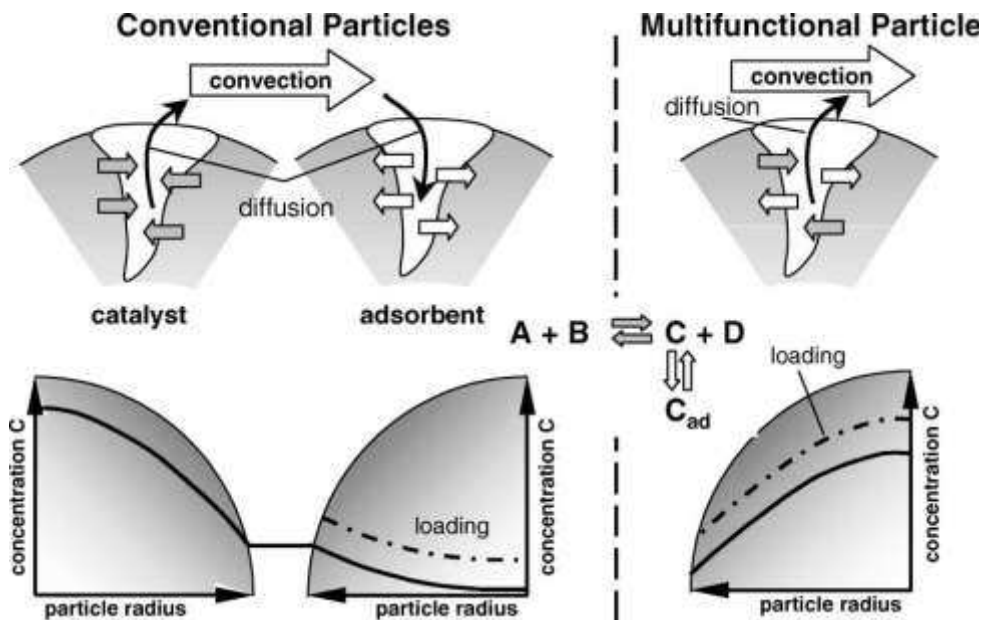
139

140 **Figure 2.** Schematic comparison of the coupling of reaction and chemisorption and the

141 resulting concentration profiles for conventional and multifunctional particles; the

142 loading profile proceeds more directly in a multifunctional particle.[19]

143 The combined function materials used in SESR processes are usually termed

144 bifunctional catalysts, bifunctional catalyst-sorbent materials or hybrid

145 materials/composites. Satrio et al.[30] were the first to synthesize core-shell pellets, with

146 sorbent (CaO) in the core surrounded by an alumina based shell incorporating a catalyst

147 (Ni). The results showed that incorporated functionalities in core shell pellets catalyzed

148 reactions of methane and propane in the presence of steam as well as removed CO_2

149 produced *in-situ*, thus demonstrating an effective merging of the two functionalities for

150 SESR. Study by Dewoolkar et al.[31] displayed that performance of a hybrid Ni/CaO and

151 Ni/HTlc was superior to conventional solid mixing of catalyst and sorbent, for exhibiting

152 longer breakthrough time (35 and 15 min of hybrid Ni/CaO and Ni/Htcl over 10 and 5

153 min of conventional mixture of same materials, respectively) and better chemisorption

154 capacity (5.7 and 0.9 mol-CO_2 kg-sorbent^{-1} of hybrid Ni/CaO and Ni/Htcl over 2 and 0.3

155 mol-CO_2 kg-sorbent^{-1} of conventional mixture of same materials, respectively).

156 Subsequent research has focused on CaO and HTlcs as sorbent candidates that mainly

157 incorporate Ni as a catalyst.

CaO-based composites

159 As mentioned earlier CaO is vulnerable to sintering and a loss in capture capacity at

160 high temperatures in cyclic SESR processes. The most common strategy to inhibit this

161 sintering and to improve durability is to use a refractory ceramic support to separate the

162 active CaO particles. Such a two phase structure can also be utilized for dispersing an

163 additional catalyst. Martavaltzi et al.[32] synthesized CaO-$Ca_{12}Al_{14}O_{33}$ and dispersed Ni

164 particles over the $Ca_{12}Al_{14}O_{33}$ phase. Incorporating chemisorption and catalysis phases

165 into a single material reduces the overall complexity of the reaction scheme. Ni can serve

166 as an additional stabilizer for CaO although too high a Ni content (> 16 wt. %) can block

167 access of CO_2 to chemisorption sites. The hybrid material produced H_2 yield of 90%

168 converting 80% of methane. Chanburanasiri et al.[33] compared Ni dispersed on Al_2O_3 and

169 CaO as SESR materials. Although the activity of Ni/CaO is lower than Ni/Al_2O_3, both

170 materials performed similarly in pre-breakthrough period, producing hydrogen of > 80%

171 purity, but at post-breakthrough period Ni/Al_2O_3 produced 70% hydrogen stream while

172 Ni/CaO could produce 65% hydrogen stream. The results imply that CaO has promise as

173 an active support. The authors also suggest that the use of Ni/CaO as a bifunctional

9

174 material can reduce material costs. Nahil et al.[34] used Ni-Mg-Al-CaO for biomass

175 gasification. This material exhibited better process stability over 20 cycles CO_2

176 capture/release compared to CaO. The highest hydrogen yield was 20.2 mmol g^{-1} of

177 biomass when 20 wt. % CaO was loaded onto Ni-Mg-Al. The presence of Ni and CaO

178 was found to affect hydrocarbon reforming and WGS reactions as catalyst and sorbent

179 respectively. Radfarnia and Iluita[35] investigated the optimal Ni loading for a bifunctional

180 Al stabilized Ni/CaO material and found out that material loaded with 25 wt.% CaO

181 exhibited the best performance for CO_2 chemisorption/desorption (9.3 mmol-CO_2 g-

182 sorbent^{-1} after 25 cycles) and for SESR of methane (99.1% methane conversion and

183 96.1% hydrogen production). In another study by the same authors[36], they used a ZrO_2

184 based support to stabilize a Ni/CaO bifunctional material and learnt that 20.5 wt. % of

185 NiO yielded best results (average H_2 yield of 89%). High Ni content also had advantage

186 of accelerated gasification of deposited coke. Ashok et al.[37] synthesized Ni/CaO-Al_2O_3

187 from HTlc derived precursors for steam reforming of biomass and model tar compound.

188 The optimum combination of Ni-Ca-Al (8:62:30) captured 3.9 mmol-CO_2 g-sorbent^{-1}

189 after 10 cycles of chemisorption/desorption. The authors observed a synergy between

190 presence of Ni and CaO phase which resulted in nearly 70% of toluene conversion and a

191 carbon deposition rate of 2.5 mg-C g^{-1} h^{-1}. Under the same compound, the biomass

192 conversion was recorded to be approximately 85% at 650 °C. Xu et al.[38] prepared

193 bifunctional materials in the form of extrudates to improve the materials' stability and the

194 most stable sorbent displayed 4 % loss in capacity after 50 cycles capturing 0.436 g-CO_2

195 g-sorbent^{-1}. As the use of a refractory support material is critical to the performance of

196 CaO as a sorbent, research effort has now focused on means for uniformly distributing a

197   catalyst within a supported structure, and its optimal loading[39]. **Table 1** summarizes the

198   performances and the operating conditions of the various materials discussed here.

199

200   **Table 1.** Synthesis method, conditions and performance of various bifunctional materials.

Material	Preparation Method	Feedstock	Conditions	SESR Cycles	H$_2$ purity	Ref.
Ni/CaO-Al$_2$O$_3$	Conical drum pelletizer	CO	600 °C, S/CO =3	N/A	H$_2$ > 97 %	40
Ni/Ca-ex-HTlc	Co-precipitation method	Methane	550 °C, S/C=4,	10	H$_2$ = 99 %	41
Ni/CaO-Al$_2$O$_3$	Wet-mixing method	Methane	650 °C, S/C=4	10	H$_2$ = 96.1%	35
Ni/CaO-Ca$_5$Al$_6$O$_{14}$	Sol-gel method	Methane	750 °C, S/C=4	10	H$_2$ > 95%	38
Ni/CaO-Zr	Wet-mixing method	Methane	650 °C, S/C=4	10	H$_2$ = 91%	36
Ni/CaO-Ca$_{12}$Al$_{14}$O$_{33}$	Soft-chemistry route	Methane	650 °C, S/C=3.4	45	H$_2$ = 90%	32
Ni/CaO	Incipient wetness method	Methane	600 °C, S/C=3	N/A	H$_2$ = 80%	33
Ni/CaO-Al$_2$O$_3$	Co-precipitation method	Ethanol	500 °C, S/C=4	10	N/A	39
Ni/Mg-HTlc	Co-precipitation method	Ethanol	300 °C, S/C=5	25	H$_2$ = 90%	42
Ni/Cu-HTlc	Co-precipitation method	Ethanol	300 °C, S/C=5	25	H$_2$ = 90%	42
K-Ni/Cu-HTlc	Wet impregnation	Ethanol	500 °C, S/C=10	N/A	H$_2$ =99.8%	43

201

202   **HTlcs-based composites**

11

203   HTlcs sorbents are a good fit for SESR of ethanol because the reforming reactions

204   can take place at an intermediate temperature range (< 500 °C) that is not detrimental to

205   the integrity of HTlcs' structure. Ethanol reforming requires high steam-to-carbon (S/C)

206   molar ratios to reduce carbon deposition and this is an energy intensive process. HTlcs

207   are regenerated when excess steam is supplied to rebuild the hydroxide structure.

208   However, an increased S/C ratio will lower the partial pressure of CO_2 produced in the

209   reactor. Partial pressure of CO_2 plays an important role in the chemisorption of CO_2 and

210   its decrease will adversely affect the performance of the sorbent. It is assumed that HTlcs

211   capture CO_2 *via* multilayer chemisorption, where multiple molecules of CO_2 can occupy a

212   single site forming a complex. Synthetic HTlcs offer versatility in the interlayer spacing

213   by tailored substitution of anions and cations.[31] The alkalinity of HTlcs is a positive

214   attribute for a CO_2 sorbent, enhancing hydrogen selectivity and reducing carbon

215   deposition.[42] HTlcs are suitable supports for catalysts too. Wu et al.[44] conducted a

216   simulated study on Ni/HTlcs (Mg^{2+}/Al^{3+} based HTlc) in SESR of ethanol under different

217   conditions to predict the performance of the materials. The optimum reaction conditions

218   were found to be a molar ratio of steam/ethanol = 10 and weight to active metal/molar

219   flow rate of ethanol = 0.25 kg h^{-1} mol^{-1} at 500 °C. Under these conditions hydrogen

220   concentrations remained over 95% for first 500 s, reaching as high as 99%. Dewoolkar

221   and Vaidya[42] prepared synthetic Ni/HTlcs by cationic modification for SESR of ethanol.

222   The metal components for cationic substitution were Mg, Ca, Cu and Zn with Cu and Mg

223   shown to be most suitable as they displayed prolonged stability (over 25 cycles), highest

224   chemisorption capacity (of 0.74 mol-CO_2 kg-$sorbent^{-1}$ and 0.42 mol-CO_2 kg-$sorbent^{-1}$ for

225   Cu and Mg based material, respectively), longest breakthrough time (25 min and 15 min

226 for Cu and Mg based material, respectively), and high hydrogen purity (95.1 mol % and

227 89.3 mol % for Cu and Mg based material, respectively) In a comparison between a

228 synthesized bifunctional material (Ni/HTlc) and a conventionally mixed Ni/Al_2O_3 with

229 HTlc,[31] the bifunctional material delivered 90% CH_4 conversion, 96.6% H_2 purity at 400

230 °C, 0.9 mol-CO_2 kg-sorbent^{-1} chemisorption, and 15 min breakthrough time in reactor.

231 The results from bifunctional material were better than the results produced by

232 conventional mixture of the phases which amounted to H_2 purity <80%, as well as lower

233 chemisorption capacity and breakthrough time (0.3 mol-CO_2 kg-sorbent^{-1} and 5 min,

234 respectively). Cunha et al. explored Cu based bifunctional material[45] and K-promoted Ni-

235 Cu bifunctional material[43] for ethanol SESR and obtained results showing > 90% H_2

236 stream for Cu/Mg-Al and 99.8% H_2 stream for K-Ni-Cu/HTlc.

237

238 **3. ALKALI METAL CERAMICS: NON-HYBRID BIFUNCTIONAL**

239   **MATERIALS**

240   So far the choice of material has been limited to the hybrid-type materials and results

241 have shown an improvement over physical mixing of separate materials, a clear

242 demonstration of the merits of bifunctional materials. CaO-based composites are always

243 in need of an inert support to overcome poor mechanical durability. The support also

244 provides additional surface area to disperse catalyst, fulfilling a dual role. But even with

245 the addition of support, CaO based materials are prone to losing performance over time.

246 HTlcs-based materials are a good match for SESR of ethanol but they are limited by

247 rapid deterioration at high temperatures (> 500 °C) ruling them out as materials for SESR

248 of methane or biomass. Alkali metal ceramics are attractive as next-generation

13

249   compounds for bifunctional materials at temperatures > 500 °C because they exhibit

250   mechanical stability, CO_2 selectivity and recyclability in these conditions Unlike CaO-

251   based sorbents, alkali metal ceramics do not require additional refractory support for

252   mechanical stability in high-temperature scenarios. Furthermore, bringing catalyst and

253   sorbent sites closer will improve the kinetics of ceramics, which remain a frailty in the

254   otherwise attractive profile of the materials. More importantly, the alkali carbonate

255   products produced on CO_2 chemisorption can provide an intrinsic catalyst role, making

256   the ceramics exempt from further engineering to introducing additional catalysts.

257   **Figure 3** illustrates a hypothetical route of progress in bifunctional alkali metal

258   catalyst/sorbent during SESR. At the start, alkali metal sorbents absorb CO_2 generated by

259   degradation of feedstock as a function of high-temperatures. The catalytic alkali metal

260   carbonate sites are yielded as a result of CO_2 capture along with secondary phases which

261   may be metal oxides or derivative phases of alkali metal ceramics depending upon the

262   sorbents. The freshly formed catalyst functions to crack and reform the hydrocarbons

263   producing more CO_2 and the desired H_2, initiating simultaneous chemisorption and

264   reforming. The process continues until all the sorbent sites on the material have been

265   turned into catalyst sites and chemisorption cannot take place any longer. The ability of

266   alkali metal ceramics to release CO_2 makes the process cyclic and alkali metal carbonates

267   show good ability for tar cracking and degradation of biomass as discussed in Section 5.

268   Multiple pathways to synthesize alkali metal ceramics offer versatility in production and

269   control over morphology which will be valuable in developing bifunctional material

270   performance.

271
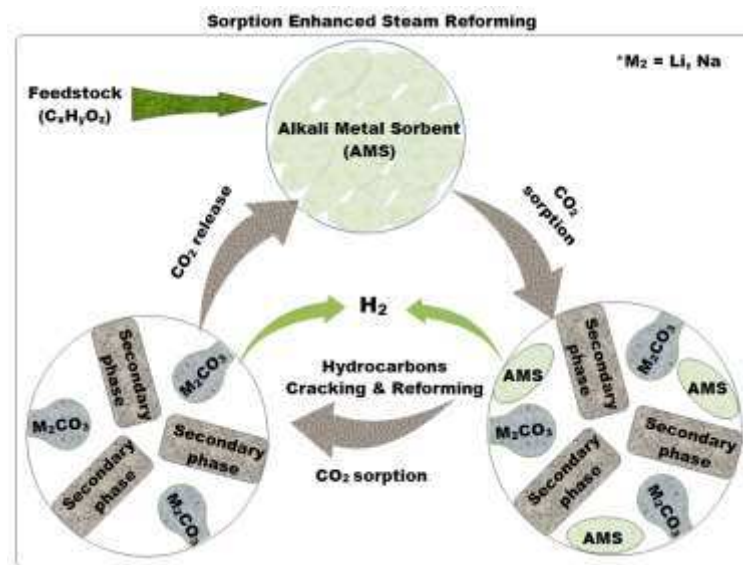
Figure 3. A hypothetical progression of alkali metal bifunctional catalyst/sorbent. The material starts as sorbent (top) and attains catalytic functionality after chemisorbing CO_2 (bottom right), which makes it capable of chemisorption and reforming simultaneously. The material becomes a catalyst after all chemisorption sites are filled (bottom left).

Alkali metal zirconates (Li_2ZrO_3, $Li_6Zr_2O_7$, Li_8ZrO_6 and Na_2ZrO_3) fit well with the requirements of a solid sorbent candidate and Li_2ZrO_3, in particular, has been extensively studied for this purpose.[25-28, 46-54] Zirconates of other alkali metals have not been identified as CO_2 acceptors, but Duan[55] carried out a first-principle density functional theory study of K_2ZrO_3 as a CO_2 sorbent to suggest that K_2ZrO_3 requires too high a temperature (> 1000 °C) to regenerate economically. Li_2ZrO_3 and Na_2ZrO_3 display excellent selectivity towards CO_2 in a gas mixture, which makes them applicable to carbon capture from a flue gas stream where CO_2 concentrations can be less than 15%. Higher Li/Zr molar ratios lead to the formation of $Li_6Zr_2O_7$ and Li_8ZrO_6, respectively.[56, 57] $Li_6Zr_2O_7$ captures over four times more CO_2 than Li_2ZrO_3 in the temperature range of

15

286　450-600 °C, owing to the greater Li content. However, after the lithium at the surface is

287　reacted, the kinetics of chemisorption slow. $Li_6Zr_2O_7$ requires CO_2 desorption

288　temperatures of over 800 °C and gradually loses its chemisorption potency during multi-

289　cycle operation due to sintering and sublimation of Li_2O.[57] Li_8ZrO_6 is not a widely

290　studied material owing to its difficult synthesis procedure.[58] Li_8ZrO_6 exhibits low uptakes

291　of CO_2 at temperatures lower than 700 °C capturing 7 mmol-CO_2 g-sorbent^{-1} in 2 hours.[57]

292　But upon reaching the melting point of Li_2CO_3 (710 °C or above) the chemisorption rate

293　significantly increases, and the sorbent can capture up to 12.2 mmol-CO_2 g-sorbent^{-1}

294　(53.98 wt. %) under 30 min.[59, 60] Similar to the case of $Li_6Zr_2O_7$, the performance of

295　Li_8ZrO_6 declines over multiple chemisorption/desorption cycles due to sublimation of

296　Li_2O.

297　　Alkali metal silicates (Li_4SiO_4, Li_8SiO_8, Li_2SiO_3 and Na_2SiO_3) are another widely

298　explored set of CO_2 sorbents. Among them Li_4SiO_4 is the promising alkali metal silicate

299　sorbent possessing the ability to trap CO_2 in the range of 450-650 °C and having a high

300　CO_2 holding capacity (up to 36.7 wt. % or 8.34 mmol-CO_2 g-sorbent^{-1}). Li_4SiO_4 has

301　exhibited fast chemisorption kinetics, good mechanical stability under multiple cycles,

302　and a low regeneration temperature range of 750-800 °C.[20, 61] The chemisorption

303　performance of Li_4SiO_4 falls between Li_2ZrO_3 and Na_2ZrO_3, but Li_4SiO_4 can be

304　synthesized from cheaper silicate precursors and it shares the same high temperature

305　performance qualities that make alkali metal zirconates desirable CO_2 sorbents.[62] It has

306　been noted that prior to utilization of Li_4SiO_4 in industrial applications for CO_2 capture,

307　the flue gas must be desulfurized as Li_4SiO_4 can irreversibly react with SO_2 to form

308　Li_2SO_4.[63] Li_8SiO_6 is a recently reported sorbent, formed as a result of high Li/Si ratio.[64]

309   Li_8SiO_6 may produce different secondary phases while reacting with CO_2 depending upon

310   its quantity. However it requires a desorption temperature of 830 °C, which will make the

311   material vulnerable to Li_2O sublimation.[65] Alkali metal metasilicates (Li_2SiO_3 and

312   Na_2SiO_3) can capture a minute amount of CO_2 (> 0.1 mmol-CO_2 g-sorbent^{-1}) with only

313   superficial reaction at relatively low temperature of 130 °C or below.[66,67] Study of

314   Na_2SiO_3 showed that the packed structure of sorbent makes it unfavorable for CO_2

315   diffusion [67]

316   Apart from the above mentioned zirconates and silicates, researchers have looked into

317   other alkali metal compounds. Lithium aluminate (Li_5AlO_4) is a lightweight polymorphic

318   ceramic possessing a very high ability to capture CO_2 at 19.8 mmol-CO_2 g-sorbent^{-1} (87.5

319   wt.%).[20] Along with promising chemisorption capacity, Li_5AlO_4 has also displayed good

320   kinetics of chemisorption, however under multicycle operation, chemisorption capacity

321   of the lithium aluminates decayed.[68] Lithium cuprate (Li_2CuO_2) is another promising

322   lightweight compound that has exhibited an ability to capture CO_2 at a wider range of

323   temperatures than other alkali metal ceramics (120-690 °C) and can remain an effective

324   CO_2 sorbent at low partial pressures of CO_2.[69, 70] Li_2CuO_2 is yet to be investigated under a

325   multicycle CO_2 capture and release process. Alkali metal titanates (Li_4TiO_4 and Na_2TiO_3)

326   can also capture CO_2 under a wide range of temperatures, 250-800 °C but regenerate

327   poorly.[71, 72] Lithium ferrite was tested and found to have insufficient capture capacity for

328   practical use as a CO_2 sorbent.[73]

329   To summarize, alkali metal ceramics possess a number of compounds that can

330   actively trap CO_2 over a wide range of temperatures (**Table 2**). Li_5AlO_4, and Li_2CuO_2

331   have shown promising results but they are in need of further studies with regards to their

332   regeneration and stability in a prolonged multi-cycle process. Li_2ZrO_3, Li_4SiO_4 and

333   Na_2ZrO_3 are the three sorbents that have been most scrutinized and display promising

334   performance indicators for a CO_2 sorbent.

335

336   **Table 2.** Characteristic performance of alkali metal materials.

Material	Chemisorption Temperature (°C)	Regeneration Temperature (°C)	Max. CO_2 chemisorption (mmol g-sorbent^{-1})	Notes
Li_4SiO_4	450-650	750-850	8.34	Qualified sorbent for bifunctional material
Li_2ZrO_3	400-600	600-800	6.52	Durable sorbent with weak kinetics
Li_2CuO_2	120-690	700-840	9.13	Promising sorbent. Needs further research with regards to durability.
Li_5AlO_4	250-800	750	19.88	High chemisorption capacity, decent kinetics, lightweight material, Weak durability
$LiFeO_2$	350-500	600-700	5.27	Weak kinetics
Li_4TiO_4	250-800	> 1000	9.54	High desorption temperature
Li_8SiO_8	300-700	830	16.7	High desorption temperature makes the material vulnerable to Li_2O sublimation
Na_2ZrO_3	500-700	800	5.4	Qualified sorbent for bifunctional material
Na_2SiO_3	30-130	--	8.2	Only Superficial reaction registered.
Na_2TiO_3	250-780	700-800	7.04	Poor regeneration.

337

338   **4. SYNTHESIS OF ALKALI METAL CERAMIC SORBENTS**

339   **Li_2ZrO_3**

340   Li_2ZrO_3 was reported as having the ability to capture CO_2 at temperatures of 450-550

341   °C by Nakagawa and Ohashi (Eqn. 4).[20]

342    $$Li_2ZrO_3(s) + CO_2(g) \rightleftharpoons Li_2CO_3(s) + ZrO_2(s), \qquad \Delta H_{298} = -160 \text{ kJ mol}^{-1} \qquad (4)$$
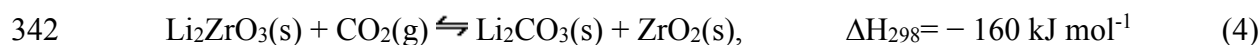
343   Li_2ZrO_3 has a theoretical maximum CO_2 chemisorption capacity of 6.5 mmol-CO_2 g-

344   sorbent^{-1} (28.7 wt. %). It captures CO_2 in the temperature range of 450-650 °C and

345   regenerates at a relatively low temperature of 700 °C. After trapping 1 mol of CO_2, the

346   volume of the material increases to 134%.[46, 48] Generally, Li_2ZrO_3 is found in two phases:

347   tetragonal (t-Li_2ZrO_3) and monoclinic (m-Li_2ZrO_3). t-Li_2ZrO_3 displays better stability,

348   faster kinetics, and higher chemisorption capacity than m-Li_2ZrO_3.[48] The performance of

349   Li_2ZrO_3 is highly dependent on the structure of the synthesized material where reduced

350   particle size, less particle agglomeration and phase purity result in increased CO_2 capture

351   efficiency, higher chemisorption rates, increased capacity and better cycle stability.

352   Compared to solid-state methods, soft-chemistry approaches can produce purer and

353   smaller sized t-Li_2ZrO_3 powder at a low synthesis temperature of 600 °C with improved

354   performance.[74] Studies suggested that at a calcination temperature of 400 °C, the

355   formation of Li_2ZrO_3 was incomplete as ZrO_2 was present alongside Li_2CO_3, whereas at

356   calcination temperature of 800 °C the m-Li_2ZrO_3 was present with larger sized

357   particles.[49, 74, 75] Soft-chemistry methods also bring forth increased CO_2 capture

358   efficiency, higher chemisorption rates, increased capacity and better cycle stability into

359   the materials.[74, 76, 77]

360   Ensuing research has explored synthesis pathways to produce powdered t-Li_2ZrO_3

361   possessing smaller particle size and minimal agglomeration.[74, 76, 78] Xiao et al.[76] reported

362   different preparation methods of the same nominal powder composition produced

363   different particle properties, leading to varied CO_2 chemisorption performances. The

364   authors also suggested that soft-chemistry methods produce heterogeneous ion

19

365 distributions resulting in uneven spatial dispersal of Li and Zr species which leads to

366 reduced CO_2 capture performance. Radfarnia et al.[78] used sonication to improve particle

367 stability during multi-cycle chemisorption/desorption. In a study by Kang et al.,[79]

368 synthesis of Li_2ZrO_3 with $Li_6Zr_2O_7$ phases was recorded following a biomimetic solution

369 route using metal containing complexes of polymeric precursors. Khokhani et al.[80]

370 synthesized Na doped Li_2ZrO_3 by citrate based sol-gel processing, using CTAB as a

371 surfactant and the product again showed high chemisorption capacity of 4.5 mmol-CO_2

372 g-sorbent^{-1} under 20 min at 650 °C and stable cyclic ability over 5 cycles. The

373 hydrothermal route has also been explored to synthesize t-Li_2ZrO_3 nanotubes with

374 enhanced CO_2 chemisorption properties over Li_2ZrO_3 nanoparticles.[58,81] **Figure 4** shows

375 SEM images of Li_2ZrO_3 particles synthesized by different methods.

376
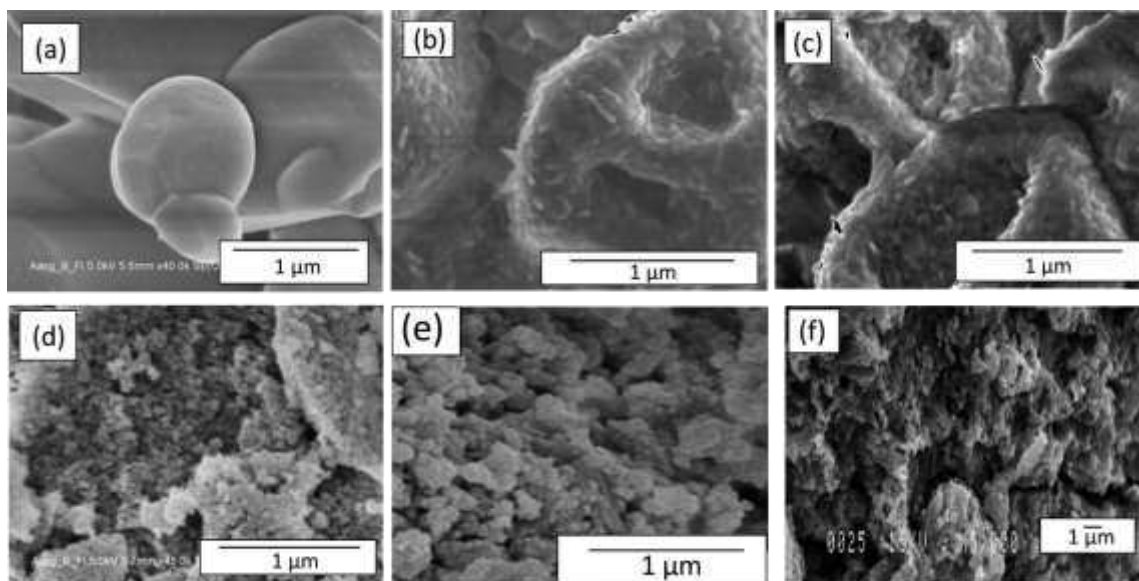
377

378 **Figure 4.** SEM images of Li_2ZrO_3 samples prepared by different methods: (a) solid

379 state reaction,[82] (b) soft-chemistry method with spray drying,[74] (c) soft-chemistry method

380 with freeze drying,[75] (d) co-precipitation method[82] (e) sol-gel method[76] and (f) surfactant

381   template with sonication assistance method.[78] Soft-chemistry, sol-gel method and co-

382   precipitation method give fine control over morphology yielding smaller particle size and

383   greater surface area which are of vital importance in helping sorbent capture CO_2 to their

384   fullest potential.

385

386   High CO_2 concentrations have proven to be beneficial for chemisorption in Li_2ZrO_3,

387   while partial pressures <0.3 bar slow down the diffusion of ions and hinder the

388   chemisorption.[78] Halabi et al.[83] studied Li_2ZrO_3 for chemisorption-enhanced auto-thermal

389   steam reforming of methane. Li_2ZrO_3 converted 99.5% of the initial methane and yielded

390   hydrogen of 99.5% purity at a temperature as low as 500 °C and pressure as low as 4.47

391   bar. The slow kinetics of chemisorption were attributed to a high concentration of

392   impurities (CO_2 and CO) in the gas effluent before the breakthrough into the transient

393   chemisorption-enhanced regime.

394   **Li_4SiO_4**

395   Li_4SiO_4 is a promising alkali metal ceramic sorbent and its reported fast

396   chemisorption kinetics have been subject to wide research interest (Eqn. 6).[61, 66]

397        $$Li_4SiO_4(s) + CO_2(g) \rightleftharpoons Li_2CO_3(s) + Li_2SiO_3(s), \quad \Delta H_{298} = -142 \text{ kJ mol}^{-1} \quad (5)$$
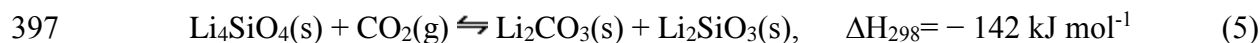
398   Li_4SiO_4 can trap CO_2 up to 30 times faster than Li_2ZrO_3 at 500 °C (20 % CO_2

399   concentration) i.e.> 50 mg-CO_2 g-sorbent^{-1}. In the same experiment Li_4SiO_4 was able to

400   capture > 5.6 mmol-CO_2 g-sorbent^{-1} in a CO_2 concentration of 2% in 50 min.[49] A

401   secondary phase of Li_2SiO_3 improves the kinetics of Li_4SiO_4, enhancing the diffusivity

402   Li^+ and O^{2-} ions even at room temperature.[84] Similar to Li_2ZrO_3 particle size is a very

21

403 important factor in the performance of the material,[85] as fine grain size results in higher

404 surface area where Li atoms can reside. **Figure 5** summarizes different routes to

405 synthesize Li_4SiO_4 and how they affect particle morphology.

406

407

408
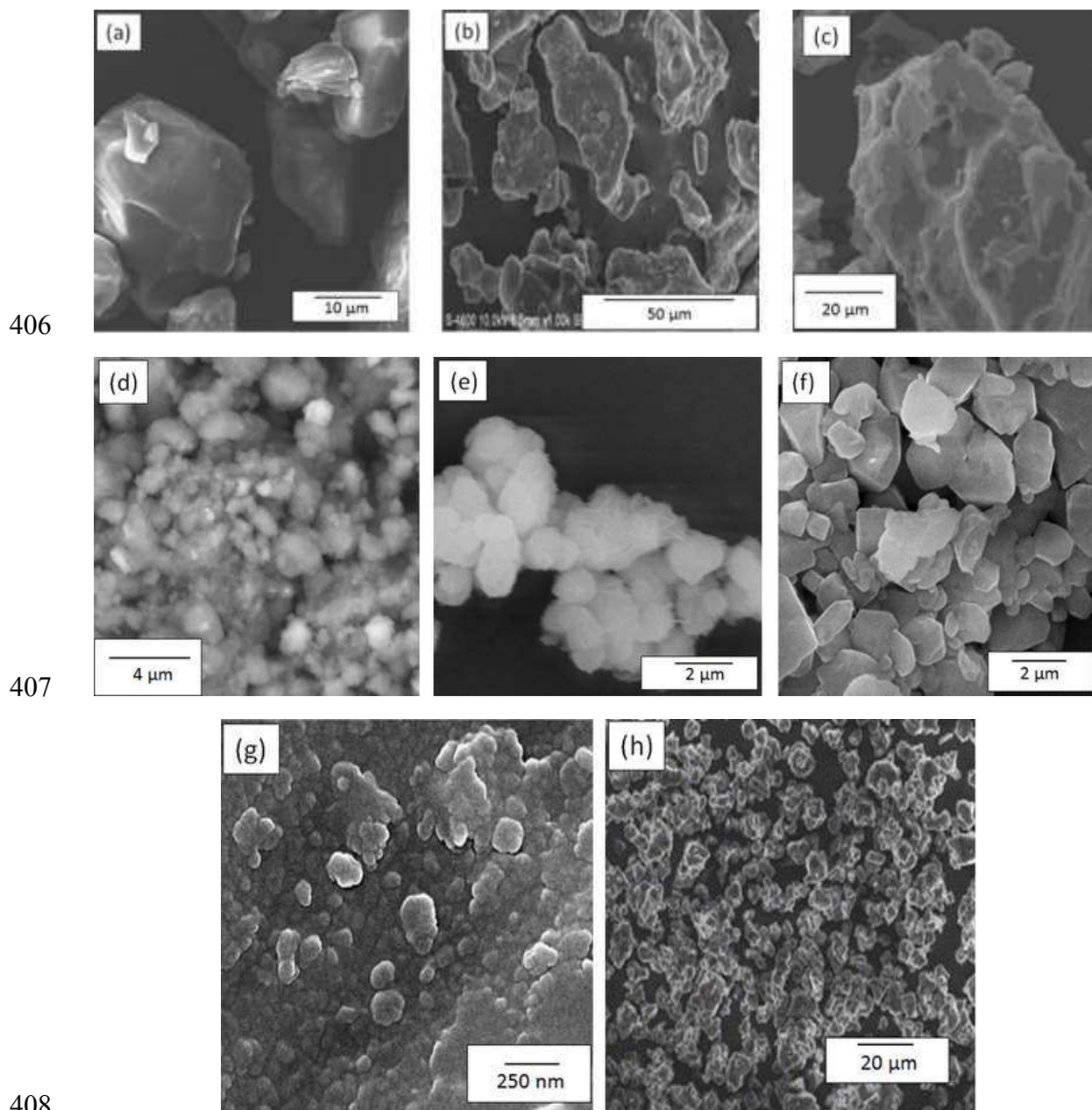
409 **Figure 5**. SEM images of Li_4SiO_4 samples prepared by different methods: (a) solid state

410 reaction,[85] (b) solid state reaction (rice ash husk sample),[86] (c) solid state reaction sample

411   before ball-milling,[87] (d) solid state reaction sample after ball-milling,[87] (e) precipitation

412   method,[85] (f) sol-gel method,[85] (g) water-based sol-gel method,[88] and (h) impregnated

413   suspension method.[89] Li_4SiO_4 particle sizes are generally found to be larger than its

414   zirconates counterpart. Sol-gel method offers a desirable mesoporous structure.

415   Silicates are generally cheaper and of lower density than zirconates and one of the

416   benefits of Li_4SiO_4 is that it can be produced from waste and existing minerals. Li_4SiO_4

417   has been synthesized from fly-ash, rice husk and diatomite, and the products have

418   exhibited desirable chemisorption properties due to the high surface area and pore

419   volume of the precursors.[86, 90-93] Wang et al.[86] used rice husk ash as a silica precursor for

420   Li_4SiO_4 synthesis. The synthesized sample displayed superior uptake performance over

421   15 cycles because the presence of impurity metals in the rice husk ash caused improved

422   reaction kinetics with CO_2 in comparison with pure Li_4SiO_4. Olivares-Marin et al.[92]

423   developed Li_4SiO_4 samples using fly-ash collected from power plants. The authors added

424   K_2CO_3 to the samples in varying ratios and results indicated 600 °C and 40 mol % K_2CO_3

425   to be optimum capture conditions under which samples were able to trap 101 mg-CO_2 g-

426   sorbent^{-1} within 15 minutes. Yang et al.[94] synthesized Li_4SiO_4 using SiO_2 colloidal

427   solutions and organic lithium precursors *via* impregnated suspension method. At the end

428   of 40 cycles of CO_2 capture and release, the performed chemisorption capacity of

429   sorbents increased from 3.2 to 5.8 mmol-CO_2 g-sorbent^{-1}. The authors attributed this

430   improvement to the micron-sized pores which were produced during CO_2 released.

431   Consequently, the sorbents had an increased area of contact to chemisorb CO_2. Wang et

432   al.[95] employed carbon coating with sol-gel method to restrict particle growth and create a

433   more porous structure during calcination. The material produced by sol-gel method is

434   required to undergo calcination to obtain Li_4SiO_4 phase, like any other synthesis method.

435   However, at high temperatures, the material is susceptible to undesired particle growth,

436   as well as, morphology deterioration. Carbon coating can act as an *in-situ* barrier for

437   particle growth and release of gases during carbonization of organic compounds

438   contribute in creating a porous structure. The resulting material was able to chemisorb 7.4

439   mmol-CO_2 g-sorbent^{-1} (32.8 wt. %) with improved chemisorption kinetics and better

440   stability over 20 cycles. In another study by Wang et al.[96] the authors used gluconic acid-

441   based carbon coating to acquired Li_4SiO_4. With addition of glucoinc acid carbon coating,

442   the sorbent nanoparticles were formed in a hollow spherical shape with small grain size.

443   The results of CO_2 chemisorption test displayed that the sorbent was able to maintain it

444   chemisorption capacity of approximately of 7.7 mmol-CO_2 g-sorbent^{-1} for 10 cycles.

445   **Na_2ZrO_3**

446   In comparison to Li_2ZrO_3 and Li_4SiO_4, Na_2ZrO_3 is a more capable CO_2 sorbent having

447   the fastest chemisorption kinetics among three (Eqn. 5).[46, 97]

448      $$Na_2ZrO_3(s) + CO_2(g) \rightleftharpoons Na_2CO_3(s) + ZrO_2(s), \qquad \Delta H_{298} = -149 \text{ kJ mol}^{-1} \qquad (6)$$
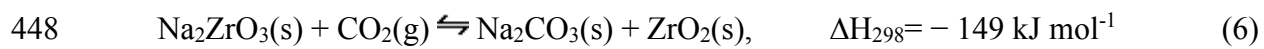
449   Na_2ZrO_3 has a theoretical maximum CO_2 uptake capacity of 5.4 mmol-CO_2 g-sorbent$^-$

450   ^{1} (23.8 wt. %), lower than both Li_2ZrO_3 and Li_4SiO_4. Na_2ZrO_3 can capture CO_2 over a

451   wide range of temperature, from room temperature to 700 °C and releases it at

452   temperature of 800 °C and above. Na_2ZrO_3 has a distinct layered structure where sodium

453   atoms are located among $(ZrO_3)^{2-}$ layers, favoring swift Na^+ ion diffusion during the bulk

454   reaction phase.[51, 98] Na_2ZrO_3 is found in two phases, namely, monoclinic and hexagonal.

455   The monoclinic phase is more reactive towards CO_2 than the hexagonal phase, owing to

456 its higher surface reactivity, stability during multi-cycle chemisorption, and effective

457 performance at low CO_2 partial pressure.[50] Soft-chemistry methods provide a purer phase

458 of Na_2ZrO_3 when the heat treatment of the sample is done *via* a two-step calcination

459 process (**Figure 6**). The selection of Na and Zr precursor compounds also has a vital

460 effect on the final morphology of the product.[99] Zhao et al.[50, 100] selected a soft-chemistry

461 route and utilized sodium citrate and zirconoxy nitrate as sources of Na and Zr,

462 respectively. The precursors formed $NaNO_3$ which has a low melting point (308 °C) and

463 that promotes diffusion of Na^+ ions throughout ZrO_2. In contrast, when zirconoxy

464 chloride and sodium acetate were used as precursors, Na_2CO_3 was formed within a

465 zirconia complex. Na_2CO_3 has a high melting point (851 °C) and subsequently does not

466 support diffusion of Na^+ ions as readily, ultimately hindering the formation of Na_2ZrO_3.
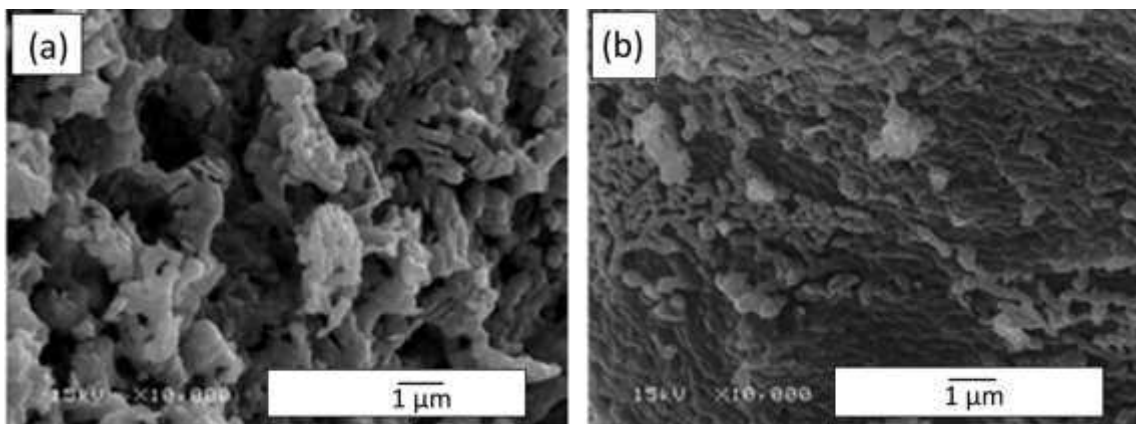
467

468 **Figure 6**. Na_2ZrO_3 samples prepared by soft-chemistry method[50] with (a) two-step

469 calcination, and (b) one-step calcination. As it can be seen from SEM images above two-

470 step approach produces a porous structure which can aid in diffusion of CO_2.

471

472 The CO_2 trapped at lower temperatures gets released at 800 °C however, the

473 desorption kinetics of Na_2ZrO_3 are slower than Li_2ZrO_3.[55] The representative synthesis

474   methods of different alkali metal ceramics and the resulting phases produced are

475   presented in **Table 3.** There is clear evidence of increased surface area after improvement

476   in synthesis routes.[78, 101]

477

478   **Table 3.** Various synthesis methods for producing alkali metal zirconates and the effects

479   on final composition.

Material	Method	Precursors	Phase	Particle size	Specific surface area $(m^2\ g^{-1})$	Refs.
Li_2ZrO_3	Solid state reaction	Zirconyl nitrate, lithium acetate	$m\text{-}Li_2ZrO_3$	_	1	101
Li_2ZrO_3	Soft-Chemistry route	Zirconyl nitrate, lithium Acetate	$t\text{-}Li_2ZrO_3$	13 nm	5	75
Li_2ZrO_3	Soft-chemistry route	Zirconyl nitrate, lithium acetate	$t\text{-}Li_2ZrO_3$	14 nm	2	102
$Na\text{-}Li_2ZrO_3$	Sol-gel	Lithium carbonate, zirconium oxychloride, CTAB, citric acid, sodium carbonate	$m\text{-}Li_2ZrO_3$	12 nm	_	80
Li_2ZrO_3	Citrate sol-gel	Zirconium(IV) oxynitrate hydrate, Lithium Nitrate , Citrate Acid, Urea	$t\text{-}Li_2ZrO_3$	17 nm	_	76
Li_2ZrO_3	Surfactant-template/ultrasound assisted method	Zirconoxy nitrate, lithium acetate (CTAB as templates)	$t\text{-}Li_2ZrO_3$	20 nm	12	78
Li_2ZrO_3	Nanotube arrays	Zirconuim foils, Lithium hydroxide	$t\text{-}Li_2ZrO_3$	_	57.9	58
Li_2ZrO_3	Liquid co-precipitation	Zirconium oxynitrate, lithium nitrate	$t\text{-}Li_2ZrO_3$	5 nm	_	82
Li_4SiO_4	Solid state reaction	Lithium carbonate, silicon dioxide	_	36 μm	_	85
Li_4SiO_4	Solid state reaction	Lithium carbonate, Si - Rice ash husk	_	16 μm	6.2	86

		(water rinsed)				
Li_4SiO_4	Solid state reaction	Lithium carbonate, Si - Rice ash husk (acid rinsed)	_	45 μm	4.6	[86]
Li_4SiO_4	Mechanical milling technique	Lithium hydroxide, silicon dioxide	_	1 – 3 μm	4.9	[87]
Li_4SiO_4	Precipitation method	Lithium acetate, tetraethyl orthosilicate	_	3 μm	_	[85]
Li_4SiO_4	Sol-gel method	Lithium hydroxide, Silicon dioxide	_	100 nm	_	[88]
Li_4SiO_4	Sol-gel method with carbon coating	Citric acid, lithium hydroxide, silicon dioxide	_	_	12.9	[95]
Li_4SiO_4	Impregnated suspension method	Lithium nitrate, silicon dioxide	_	_	> 1	[89]
Li_4SiO_4	Impregnated suspension method	Lithium lactate, silicon dioxide	_	1-6 nm	2.09	[94]
Li_4SiO_4	Impregnated suspension method	Lithium acetate dehydrate, silicon dioxide	_	1-6 nm	1.65	[94]
Na_2ZrO_3	Solid state reaction	Sodium carbonate, zirconium oxide	m-Na_2ZrO_3	150~400 nm	3.6	[53]
K-Na_2ZrO_3	Solid state reaction	Sodium carbonate, zirconium oxide, potassium carbonate	m-Na_2ZrO_3	500~800 nm	1.1	[103]
Na_2ZrO_3	Soft-chemistry route	Sodium Citrate, Zirconium(IV) oxynitrate hydrate	m-Na_2ZrO_3	30 nm	4	[50]

5. USE OF ALKALI METALS IN CATALYSIS

The evidence of catalytic activity of Na_2ZrO_3 was reported by Alcantar-Vazquez et al.,[21] where CO was catalytically oxidized into CO_2 and chemisorbed at $T \geq 200$ °C with the processes apparently taking place simultaneously. Li_2CuO_2[104], $NaCoO_2$[105] and Li_2ZrO_3[106] were also reported to perform catalytic CO oxidation to CO_2 and subsequent chemisorption of CO_2. The CO-CO_2 conversion in Li_2CuO_2 and $NaCoO_2$ follows a

486 double reaction Mars-van Krevelen mechanism. [104, 105] A study on CO oxidation ability

487 of Li_2ZrO_3 and Na_2ZrO_3 reported that Na_2ZrO_3 performed better as a CO Oxidation

488 catalyst than Li_2ZrO_3, achieving 100% CO conversion while Li_2ZrO_3 was able to only

489 convert 35% CO under similar experimental conditions (CO conversion isotherm were

490 conducted at temperature range of 30-850 ^oC with 5 vol.% CO and 5 vol.% O_2). Results

491 showed that a lower concentration of O_2 (3 vol.%) is unable to achieve full CO

492 conversion, which implies that in case of Na_2ZrO_3 the presence of oxygen for CO

493 conversion is necessary. As a contrast, CO conversion with $NaCoO_2$ was thought to be

494 aided by oxygen present in the structure of the $NaCoO_2$. Furthermore, a comparison

495 between typical Na_2ZrO_3-CO_2 chemisorption process and Na_2ZrO_3-CO-O_2 chemisorption

496 system shows that the former system displays better chemisorption performance than

497 letter. Na_2ZrO_3-CO-O_2 system cannot completely chemisorb CO_2 that is produced by

498 catalysis due to low CO_2 concentration and kinetics of CO oxidation.[106] Mendoza-Nieto

499 et al.[107] reported that carbonated Na_2ZrO_3 having Na_2CO_3-ZrO_2 phase can reform

500 methane through dry reforming process to produce syngas (H_2 + CO). Role of carbonated

501 Na_2ZrO_3 is to supply CO_2 via desorption at high temperatures (> 750 ^oC) to initiate dry

502 reforming of methane and it may act as a catalyst for the reforming process.

503   Alkali metal carbonates have shown capacity of catalysis in CO_2 gasification and are

504 able to decrease the activation energies of CO_2 gasification. Their capacity of catalysis is

505 listed from weak to strong in the following order: Li<Na<K<Rb<Cs.[108] Alkali carbonates

506 have also exhibited catalysis activity on the steam gasification of bitumen coke. Alkali

507 metal carbonates Na_2CO_3 and K_2CO_3 along with KCl, $CaCO_3$, CaO and MgO were tested

508 for steam gasification under temperature range of 600-800 ^oC. The carbonates displayed

509   the best results achieving near complete conversions for Na_2CO_3, 95.6% and K_2CO_3,

510   99.3%. The carbonates were effective because they were mobile on the coke material. In

511   the resulting product stream, little trace of CO was found which suggested that carbonate

512   catalyst strongly promoted WGS reaction.[109] Alkali metal carbonates are able to catalyze

513   Boudouard reaction on coal char and graphite, although with different kinetic parameters

514   for each material.[110] A study on catalytic effect on Li, Na and K carbonates on graphite in

515   the presence of water vapor showed that catalyzed reaction increased in the temperature

516   ranges of melting points carbonates.[111] Binary and ternary eutectic carbonate catalysts

517   have exhibited more catalytic activity than a single alkali carbonate could on coal char

518   samples. Similarly ternary eutectic carbonate catalyst is more reactive than a binary

519   eutectic carbonate catalyst. The lowered melting points of eutectic salts were believed to

520   be reason behind increased reactivity, as they enhanced the mobility of the catalyst

521   composite on the coal chars.[112, 113]

522   Alkali metals are shown to be effective in tar removal during gasification of biomass.

523   Na and K carbonates within biomass show little or no carbon deactivation and slight

524   particle agglomeration. The method of catalyst addition to feedstock through dry mixing

525   or impregnation does not lend itself to recovery of the primary catalyst and does associate

526   with a high yield of ash content.[8] Mudge, et al.[22] have also shown potassium carbonate to

527   be an effective catalyst for conversion of wood into syngas.

528   Potassium and sodium are present in biomass and their presence significantly

529   influences the degradation temperature, degradation rate and the yield of products during

530   pyrolysis.[23] Smets, et al.[114] used Na_2CO_3 as a primary catalyst along with γ-Al_2O_3 and

531   hexagonal zeolite surface modified to contain 5 angstrom pores (HZSM-5) as secondary

532 catalysts for slow pyrolysis of rapeseed cake. During pyrolysis, Na_2CO_3 converted fatty

533 acids into aliphatic hydrocarbons and reduced the organic compounds by 27.19 wt. %.

534 Na_2CO_3 ranked second among the three catalysts (highest yield was acquired with the use

535 of HZSM-5; 44.9 wt. %), however the product produced by Na_2CO_3 had the highest

536 calorific value of 36.8 MJ kg^{-1}. The presence of K_2CO_3 in the biochar for hydrothermal

537 gasification increases the gasification rate and hydrogen yield.[115]

538   Alkali carbonates are also active in decomposition of alcohols and carboxylic acids,

539 and can catalyze the water-gas shift reaction in the presence of steam at 600 °C during

540 biomass gasification. However, under the same conditions, simple chains of

541 hydrocarbons remain unaffected, as do aldehydes and ketones. K_2CO_3 performed better

542 than Na_2CO_3 during catalytic reforming of methane at temperatures higher than 800 °C.[8]

543 Alkali metal carbonates are also reported to be effective at converting condensed carbon

544 liquids into gases.[116-118] Na_2ZrO_3 was used as a catalyst for transesterification of soybean

545 oil to produce biodiesel and the results displayed a 98.3% Fatty Acids Methyl Esters

546 (FAME) conversion rate.[24] These separate studies also indicate that the alkali metal

547 carbonates can efficiently be used for diverse catalytic chemical transformations.

548 **6. CHEMISORPTION OF CO_2 BY VARIOUS ALKALI METAL CERAMICS**

549   Interactions between alkali metal ceramics and CO_2 over the course of chemisorption

550 process have been extensively studied and consequently the mechanism of CO_2

551 chemisorption over alkali metal ceramics is well understood.[119, 120] The basic nature of

552 alkali metal ceramics makes it possible for the chemisorption of CO_2, which is acidic, to

553 occur on the material. CO_2 chemisorption can be distinguished into two steps. First is a

30

554   superficial reaction phase, where alkali metal available on the surface of the material

555   reacts with CO_2. Superficial reaction can occur at different temperatures for different

556   alkali compounds, i.e. Li_2ZrO_3 captures CO_2 above 400 °C, while Na_2ZrO_3 begins

557   superficial chemisorption at over 100 °C. The result is formation of alkali carbonate shell

558   along with unreacted metal oxide or secondary alkali metal phase.

559   Second is bulk diffusion phase which is initiated by diffusion of Li/Na and oxygen

560   atoms from the unreacted core to the surface to continue the chemisorption. The majority

561   of chemisorption taking place occurs via the bulk diffusion phase and diffusion of atoms

562   in this process is the rate limiting step of the reaction. Formation of Li/Na carbonate at

563   the surface of the sorbent cause vacancy formation which is filled by diffusion of Li/Na

564   and oxygen atoms from the interior of the material to the surface. Research has shown

565   that manufacturing vacancies causes improvement in the CO_2 chemisorption rates at low

566   temperatures.[20, 121] Ortiz-Landeros et al.[119] analyzed the effects of the presence of metal-

567   oxides and secondary lithium phases during chemisorption in lithium ceramics. Li_2CO_3

568   can exist along with a metal oxide phase (ZrO_2) or with a secondary lithium phase

569   (Li_2SiO_3) after chemisorption according to eqns. (4) and (5), respectively. The metal

570   oxide phase (ZrO_2) limits the chemisorption process by acting as a barrier for the

571   diffusion. On the other hand, the behavior of secondary lithium phase (Li_2SiO_3) in

572   diffusion process depends upon its lithium diffusion coefficient. If the lithium diffusion

573   coefficient is higher than Li_2CO_3's, the CO_2 diffusion will be enhanced. A secondary

574   lithium phase with much lower diffusion coefficient than Li_2CO_3 can pose hindrance for

575   CO_2 diffusion (**Figure 7**).

31
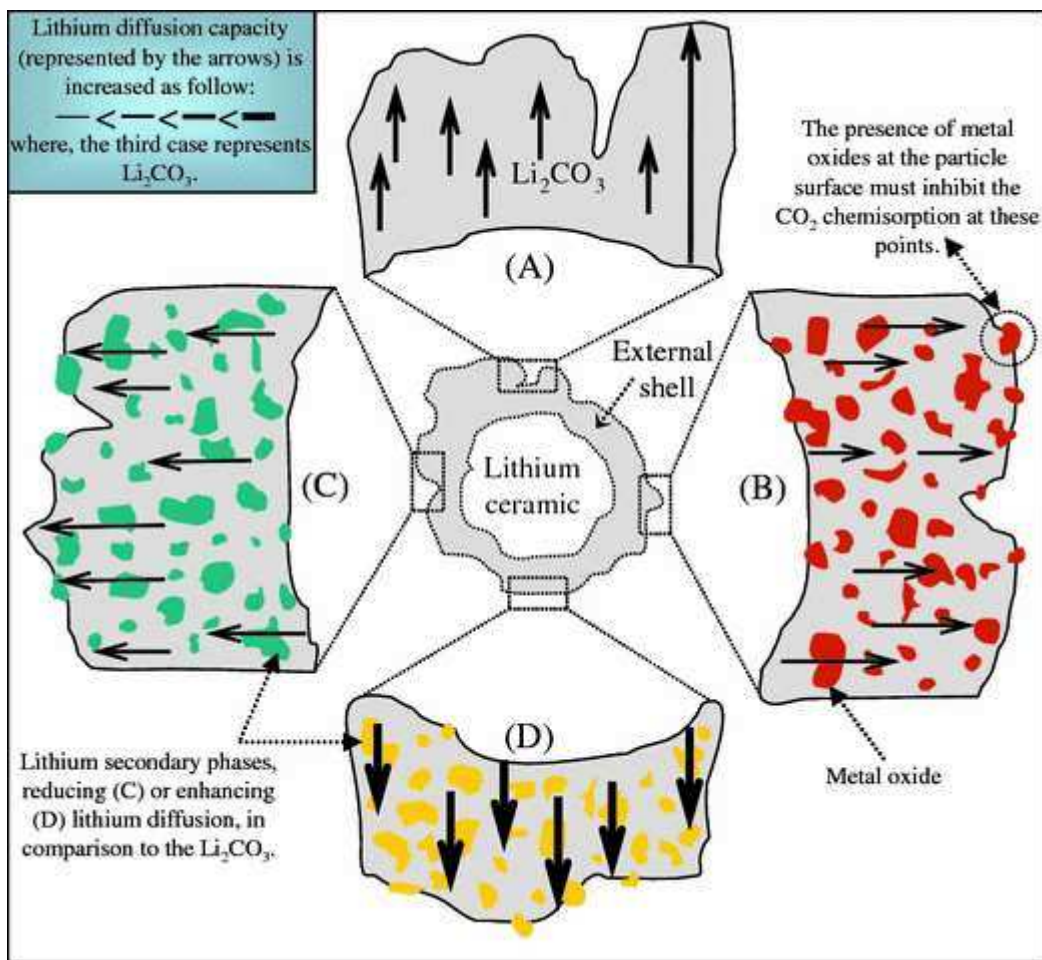
Figure. 7 The effects of metal-oxides secondary lithium phases during chemisorption

process. (A) Lithium diffusion controlled by Li_2CO_3 only, (B) lithium diffusion being

limited by metal oxide phase, (C) lithium diffusion being reduced by secondary lithium

phase, having lesser lithium diffusion coefficient than Li_2CO_3 and (D) lithium diffusion

being enhanced by secondary lithium phase having higher lithium diffusion coefficient

than Li_2CO_3 [119]

At the temperature range of room temperature to 300 °C, Na_2ZrO_3 is able to

chemisorb CO_2 *via* superficial reaction. However, the capacity and rate of chemisorption

is not uniform across the temperature range. The sorbent can capture 3.8 mmol-CO_2 g-

sorbent in 5 hrs. at 150 °C, while at 250 °C the sorbent was able to capture 0.9 mmol-CO_2

587 g-sorbent. This phenomenon can be attributed to thermal shock due to rapid heating,

588 which causes sintering that reduces the surface area[51] or another possibility is desorption

589 of CO_2 is activated and an equilibrium is reached between CO_2 chemisorption-desorption

590 which results in lowered chemisorption.[98]. A study by Martinez-dlCruz and Pfeiffer[53]

591 revealed that the sintering effect does exist however it is not caused by sintering of the

592 ceramic itself but due to changes in textural properties of the external Na_2CO_3-ZrO_2 shell

593   Na_2ZrO_3 possess higher kinetics of chemisorption than its lithium based counterparts.

594 Not only does Na have higher reactivity towards CO_2, but Na_2ZrO_3 has a lamellar

595 structure which enables better diffusion kinetics.[122] The time required for desorption is

596 dependent upon temperature; higher temperatures leads to faster desorption kinetics.[74]

597 Li_4SiO_4 displays superior regeneration ability than Li and Na zirconates, having faster

598 desorption kinetics than Li_2ZrO_3 and lower regeneration temperature than Na_2ZrO_3.[55, 97]

599 Temperature also influences the equilibrium partial pressure of CO_2 for

600 chemisorption/desorption. At low CO_2 concentrations, effective removal of CO_2 will be

601 favorable under low temperatures.[82] **Tables 4** summarizes the CO_2 capture performance

602 under different operating conditions.

603

604 **Table 4.** Multi-cycle CO_2 chemisorption performance of alkali metal ceramics under

605 varying conditions.

Material	Cycles	Chemisorption conditions	First cycle chemisorption (mmol-CO_2 g-sorbent^{-1})	Last cycle chemisorption (mmol-CO_2 g-sorbent^{-1})	Desorption conditions	Ref.

Li_2ZrO_3	3	550 °C, 100% CO_2, 200 ml min^{-1}, 20 min	5.9	5.9	690 °C, 100% N_2, 200 ml min^{-1}, 10 min	[82]
Li_2ZrO_3	3	550 °C, 100% CO_2, 0.5 bar, 40 ml min^{-1}, 60 min	5.9 within 20 min	5.9	700 °C, 100% N_2, 40 ml min^{-1}, 60 min	[76]
$K-Li_2ZrO_3$	4	550 °C, 0.25 bar, 40 ml min^{-1}, 60 min	5.1	5.1	675 °C, 100% N_2, 40 ml min^{-1}, 50 min	[123]
$Li_6Zr_2O_7$	3	800 °C, 100% CO_2, 100 ml min^{-1}, 60 min	2.7	2	900 °C, 100% N_2, 100 ml min^{-1}, 60 min	[57]
Li_8ZrO_6	4	800 °C, 100% CO_2, 100 ml min^{-1}, 30 min	7.9	5.3	900 °C, 100% N_2, 100 ml min^{-1}, 60 min	[57]
Li_4SiO_4	5	700 °C, 100% CO_2, 60 min	7.9	7.9	850 °C, 100% N_2, 30 min	[66]
Li_4SiO_4	50	600 °C, 20 % CO_2, 300 ml min^{-1}, 60 min	6.3	4.5	800 °C, 100 % N_2, 300 ml min^{-1}, 60 min	[124]
Li_4SiO_4	5	650 °C, 100% CO_2, 60 min	5	5.7	750 °C, 100 % He, 30 min	[121]
Li_4SiO_4	40	550 °C, 15% CO_2, 30 min	3.2	5.8	750 °C, 100 % N_2, 10 min	[94]
Li_4SiO_4	20	680 °C, 100% CO_2, 15 min	7.4	7.4	800 °C, 100% N_2, 10 min	[95]
Li_4SiO_4	10	665 °C, 100% CO_2, 30 min	7.7	7.6	800 °C, 100% N_2, 20 min	[96]
$LiSiO_4$	15	650 °C, 100 % CO_2, 1 L min^{-1}, 15 min	5.5	5.0	800 °C, 100 % N_2, 1 L min^{-1}, 10 min	[86]
Li_4SiO_4 - Diatomite	16	700 °C, 50% CO_2, 20 min	7.7	6.2	700 °C, 100% N_2, 30 min	[90]
Li_4SiO_4 - Diatomite	10	700 °C, 50% CO_2, 20 min	7.8	7.3	700 °C, 100% N_2, 30 min	[91]
$LiSiO_4$ – Rice Husk Ash	15	680 °C, 100 % CO_2, 1 L min^{-1}, 15 min	6.9	6.4	800 °C, 100 % N_2, 1 L min^{-1}, 10 min	[93]
$LiSiO_4$ – Rice Husk Ash	15	650 °C, 100 % CO_2, 1 L min^{-1}, 15 min	7.7	7.5	800 °C, 100 % N_2, 1 L min^{-1}, 10 min	[86]
$LiSiO_4$ – Rice Husk	15	650 °C, 100 % CO_2, 1 L min^{-1}, 15 min	7.7	7.5	800 °C, 100 % N_2, 1 L min^{-1}, 10	[86]

Ash

						min
Li$_{3.7}$Al$_{0.1}$SiO$_4$	5	650 °C 100% CO$_2$, 60 min	5	3.1	750 °C, 100 % He, 30 min	[121]
Li$_4$SiO$_4$ (2 % wt. Li$_2$ZrO$_3$)	50	600 °C, 20 % CO$_2$, 300 ml min^{-1}, 60 min	6.3	4.8	800 °C, 100 % N$_2$, 300 ml min^{-1}, 60 min	[124]
Li$_4$SiO$_4$ (5 % wt. Li$_2$ZrO$_3$)	50	600 °C, 20 % CO$_2$, 300 ml min^{-1}, 60 min	6.3	5.8	800 °C, 100 % N$_2$, 300 ml min^{-1}, 60 min	[124]
Na$_2$ZrO$_3$	20	500 °C , 100 %CO$_2$, 60 ml min^{-1}, 30 min	3.9	3.9	800 °C, 100% N$_2$, 60 ml min^{-1}, 30 min	[54]
Na$_2$ZrO$_3$	20	550 °C , 100 %CO$_2$, 60 ml min^{-1}, 30 min	4.2	4.2	800 °C, 100% N$_2$, 60 ml min^{-1}, 30 min	[54]
Na$_2$ZrO$_3$	20	600 °C , 100 %CO$_2$, 60 ml min^{-1}, 30 min	4.4	4.1	800 °C, 100% N$_2$, 60 ml min^{-1}, 30 min	[54]
Na$_2$ZrO$_3$	20	700 °C , 100 %CO$_2$, 60 ml min^{-1}, 30 min	4.8	4.2	800 °C, 100% N$_2$, 60 ml min^{-1}, 30 min	[54]
Na$_2$ZrO$_3$	20	800 °C , 100 %CO$_2$, 60 ml min^{-1}, 30 min	5	3.1	800 °C, 100% N$_2$, 60 ml min^{-1}, 30 min	[54]
K-Na$_2$ZrO$_3$	8	400 °C	2	0.7	850 °C	[103]
Na$_2$(Zr$_{1-x}$Al$_x$)O$_3$	20	550 °C, 60 ml min^{-1},30 min	4	4.3	800 °C, 100% N$_2$	[98]

606

607 **Influence of steam on CO$_2$ absorption**

608   Na$_2$ZrO$_3$ has the ability to hold water. The reaction between CO$_2$ and water-laden

609 Na$_2$ZrO$_3$ produces sodium bicarbonate (NaHCO$_3$) along with ZrO$_2$. With the formation of

610 NaHCO$_3$, the ability of Na$_2$ZrO$_3$ to capture CO$_2$ increases two fold compared to dry

611 conditions (theoretical maximum of 10.8 mmol-CO$_2$ g-sorbent^{-1}). Santillan-Reyes et al.[52]

612 reported 5.8 mmol-CO$_2$ g-sorbent^{-1} or 35 wt. % of sorbent at the temperature of 60 °C

613 under water saturated conditions. A temperature of 60 °C is too low for the activation of

614   Na diffusion, therefore the increased activity can be attributed to the availability of water.

615   The maximum capacity of CO_2 chemisorption in m-Na_2ZrO_3 is reached in less than 30

616   seconds under the influence of 10% concentrations of steam, which is over three times

617   faster than that in dry conditions.[125] Li_2ZrO_3 also displays increased chemisorption

618   kinetics under wet conditions that are likely to be found in SMR, i.e. steam

619   concentrations > 20%.[82]

620   Multiple studies have suggested that Li_2ZrO_3 and $LiSiO_4$ are capable of producing

621   over 87 vol. % H_2 in SESMR conditions and Na_2ZrO_3 led to production of 92.2 vol. % H_2

622   in SESR of ethanol.[25-28] Steam might affect mobility of alkali ions as it lowers surface

623   free energy making them likely to move towards a surface and ease the reaction with

624   CO_2.[102] Steam is also reported to enhance CO_2 diffusion through the layer of carbonate

625   formed over Li_2ZrO_3 and Li_4SiO_4.[82, 120] However, it does cause a continuous deactivation,

626   diminishing the capacity of the acceptor due to phase segregation, sintering, and/or

627   vaporization of alkali metals after forming hydro-oxides in the presence of steam.

628   Capture kinetics, regeneration and stability of Li_2ZrO_3, K-doped Li_2ZrO_3, Na_2ZrO_3, and

629   Li_4SiO_4 under steam laden conditions were tested and the results showed that capture

630   kinetics were considerably improved with 10% steam concentrations.[125] Similarly, the

631   regeneration kinetics also showed improvement under the presence of steam except for

632   Li_4SiO_4 which did not display any significant change.

633   Potassium salts/oxides are hygroscopic and their addition to Li_2ZrO_3 will increase the

634   tendency to trap water in the modified sorbent. Martinez-dlCruz, et al.[101] suggested that

635   K-Li_2ZrO_3 does not only trap water through chemisorption, but also through the reaction

636   between K-Li_2ZrO_3 and water, forming hydroxyl species. Prepared samples gained

637   weight due to hydroxylation and carbonation processes in the temperature range of 30-80

638   °C.

Influence of partial pressure

640   In operational conditions the partial pressure of CO_2 will rarely exceed 0.2 bar, which

641   makes chemisorption performance of sorbent in low partial pressure conditions a vital

642   parameter. The CO_2 in alkali metal sorbents is governed by its diffusion within the

643   sorbents and not all alkali metal sorbents are able to exhibit uniform performance at

644   different partial pressure of CO_2. Chemisorption of Li_2ZrO_3 is severely affected by the

645   low partial pressure, as reported by multiple studies.[76-78] At low partial pressures mass

646   transfer limitations inhibit the CO_2 diffusion. In these conditions CO_2 will react with Li^+

647   atoms available at the surface and form up a barrier of Li_2CO_3-ZrO_2 preventing CO_2

648   diffusion.[82] Li_4SiO_4 presents a superior chemisorption performance than Li_2ZrO_3 at low

649   partial pressures (5.9 mmol-CO_2 g-sorbent^{-1} at 0.2 bar within 30 min and 6.1 mmol-CO_2

650   g-sorbent^{-1} at 0.02 bar within 50 min).[124] Unlike Li_2ZrO_3, Li_4SiO_4 has smaller grain sizes

651   which chemisorb CO_2 at a faster rate.[49] Due to its smaller grain size, the layer of Li_2CO_3-

652   ZrO_2 formed after chemisorption is much thinner and consequently a lesser obstruction

653   for CO_2 diffusion at low partial pressures. Na_2ZrO_3 has higher surface reactivity towards

654   CO_2, particularly its m-Na_2ZrO_3 phase, which enables it to retain its chemisorption

655   capacity at low partial [50] The performance of alkali metal sorbents synthesized by at low

656   partial pressures as reported different authors is given in **Table 5.**

657

658　**Table 5.** Chemisorption performance of alkali metal sorbents under different CO_2 partial
659　pressure conditions.

Material	Chemisorption Conditions	CO_2 chemisorbed (mmol-CO_2 g-sorbent^{-1})	Refs.
Li_2ZrO_3	1.0 bar CO_2, 575 °C	5 within 20 min	[78]
Li_2ZrO_3	0.75 bar CO_2, 575 °C	4.6 in 25 min	[78]
Li_2ZrO_3	0.50 bar CO_2, 575 °C	1.1 in 25 min	[78]
Li_2ZrO_3	0.25 bar CO_2, 575 °C	0.2 in 25 min	[78]
Li_2ZrO_3	0.10 bar CO_2, 575 °C	0.1 in 25 min	[78]
Li_4SiO_4	0.20 bar CO_2, 500 °C	5.9 in 30 min	[124]
Li_4SiO_4	0.02 bar CO_2, 500 °C	6.1 in 50 min	[124]
Na_2ZrO_3	0.1 bar CO_2, 575 °C	3.86 within 10 min	[50]
Na_2ZrO_3	0.075 bar CO_2, 575 °C	3.6 in 40 min	[50]
Na_2ZrO_3	0.050 bar CO_2, 575 °C	3.6 in 40 min	[50]
Na_2ZrO_3	0.025 bar CO_2, 575 °C	3.6 in 40 min	[50]

660

661　**7. ATTEMPTS TO IMPROVE THE INHERENT CO_2 CHEMISORPTION**
662　　**CAPACITY OF ALKALI METAL CERAMICS**

663　**Effect of carbonate salts**

664　　During alkali metal ceramic carbonation, CO_2 diffusion through the solid carbonate

665　outer shell occurs at temperatures below 600 °C. Addition of carbonate salts to form a

666　molten carbonate shell at these temperatures will enhance diffusion of CO_2 and

667　effectively increase the chemisorption range (**Table 6**).[60, 75] Furthermore, alkali metal

668　carbonate additions can form a molten salt ternary mixture which displayed a 2 mg g^{-1}

669　min^{-1} chemisorption rate at a low temperature of 450 °C.[49] It is reported that K-promoted

38

670 chemisorption improves kinetics in the diffusion of CO_2 through the bulk, but the surface

671 reaction chemisorption kinetics remain the same.[9]

672   Apart from CO_2 diffusion, molten carbonate eutectic phase mixtures change the

673 viscoelastic properties of the sorbent mixture i.e. materials display more liquid-like

674 characteristics. It is reported that molten carbonate phases require a heating rate of > 10

675 °C min^{-1} to alter the viscoelastic properties and enhance the amount of molten carbonate

676 phase whereas a lower heating rate aids chemisorption and diffusion of CO_2 throughout

677 the sorbent. However, mass transfer at a heating rate of > 10 °C min^{-1} limits CO_2

678 diffusion and, in this instance, formation of a molten phase prevails over diffusion of

679 CO_2.[126]

680

681 **Table 6.** Composition and eutectic temperatures of binary and ternary eutectic mixtures

682 of carbonate salts studied by thermogravimetric analyzers.[127]

Eutectic salt composition (mol %)	Melting point (°C)
K_2CO_3 38%, Li_2CO_3 62%	488
K_2CO_3 57.3%, Li_2CO_3 42.7%	498
Na_2CO_3 48%, Li_2CO_3 52%	500
KF 38%, Li_2CO_3 62%	N/A
K_2CO_3 57%, $MgCO_3$ 43%	460
K_2CO_3 26.85%, Na_2CO_3 30.6%, Li_2CO_3 42.5%	393
K_2CO_3 16.4%, Na_2CO_3 26.4%, Li_2CO_3 57.1%	372
KCl 36.8%, NaCl 36.2%, Na_2CO_3 27 %	560
K_2CO_3 42%, NaF 32%, Na_2CO_3 26%	562
NaCl 31%, Na_2CO_3 54%, NaF 15%	575

683

684

Influence of doping on CO_2 chemisorption

The doping of Li_2ZrO_3 with K can change the melting point and create an eutectic shell that becomes liquid at lower temperature, which significantly improves the CO_2 diffusion rate and provides better CO_2 chemisorption than a solid carbonate shell. K-doped Li_2ZrO_3 shows faster kinetics of chemisorption in the presence of a molten eutectic phase, the limiting step of the reaction becomes the diffusion of Li^+ ions and O^{2-} ions in place of CO_2 in the solid phase of an undoped Li_2ZrO_3.[48, 60, 126-128]. However, this addition of potassium will adversely affect the equilibrium chemisorption capacity of the sample. $K_{0.2}Li_2Zr_{3.1}$ can theoretically capture 6.1 mmol-CO_2 g-sorbent^{-1}, but increasing K amount to $K_{0.6}Li_2Zr_{3.3}$ will lower the theoretical capture capacity to 5.5 mmol-CO_2 g-sorbent^{-1}. $K_{0.2}Li_{1.6}ZrO_{2.9}$ was found to be optimum ratio where the material captured 5.7 mmol-CO_2 g-sorbent^{-1} in under 15 minutes.[123] Gauer and Heschel[121] improved the performance of Li_4SiO_4 by doping the material with Al and Fe and creating vacancies inside the structure to facilitate improved chemisorption. Compared with K-doped Li_4SiO_4, which provides good chemisorption at lower temperatures but requires higher temperatures to regenerate, vacancy doped material, particularly Fe > Al, provides improved reactivity 500 °C. It should also be noted that $Li_{3.7}Al_{0.1}SiO_4$ and $Li_{3.7}Fe_{0.1}SiO_4$ performed similarly in chemisorption but desorption of $Li_{3.7}Al_{0.1}SiO_4$ was incomplete while $Li_{3.7}Fe_{0.1}SiO_4$ completed desorption at 750 °C. It is because Fe will form a weaker oxygen bond in comparison with Al atoms, therefore O^{-2} ion diffusion is relatively unhindered by $Li_{3.7}Fe_{0.1}SiO_4$ resulting in complete desorption. Seggiani et al.[129] tested Li_4SiO_4 silicates samples doped with different carbonates at varying concentrations. The doped samples performed better than pure Li_4SiO_4 however, the samples were subject to decay after the

708 first chemisorption/regeneration cycle due to sintering. The sample with 30% K_2CO_3-

709 doped Li_4SiO_4 remained most stable after 25 cycles with only 4 wt. % loss of capture

710 capacity along with displaying best chemisorption performance in terms of kinetics and

711 chemisorption capacity of 3.4 mmol-CO_2 g-sorbent^{-1}.

712   Addition of potassium to Na_2ZrO_3 also noticeably improves the chemisorption

713 kinetics of the material as a K-Na eutectic salt is formed. Again the low-temperature

714 molten carbonate phase enhances the diffusion of the CO_2. However, thermal and cyclic

715 stability of the sorbent is affected due to potassium sublimation during high-temperature

716 desorption.[103] K-doped Na_2ZrO_3 favors chemisorption at much lower temperature (400

717 °C).[103]

718   Dissolved aluminum in sodium zirconates produces $Na_2(Zr_{1-x}Al_x)O_3$ ($x \leq 0.3$).[98]

719 Aluminum oxide addition gives improvements in CO_2 capture during the surface

720 chemisorption phase, and the $Na_2(Zr_{1-x}Al_x)O_3$ exhibits peak CO_2 capture at 600 °C (4

721 mmol-CO_2 g-sorbent^{-1}; in contrast to Na_2ZrO_3 which displays its peak performance at 550

722 °C). 600 °C is the temperature at which the Na_2CO_3 outer shell densifies in Na_2ZrO_3

723 sorbents. Improved performance at 600 °C indicates that aluminum oxide addition

724 provides resistance to sintering and densification at 600 °C. These solid solutions have

725 good stable cycle stability.

726   Doping of Li into Na_2ZrO_3 is more favorable for chemisorption than doping with

727 K[130]. Increasing Li as a dopant will lower regeneration temperature for Na_2ZrO_3 and

728 enhance the stability of the structure, whereas similar increments of K as a dopant will,

729 on the whole, increase the regeneration temperature and adversely affect the structure.

41

8. OUTLOOK

The concept of bifunctional catalyst-sorbent is a logical progression in the field of SESR, on account of advantages offered such as reduced cost and improved mass transfer over conventional sorbent and catalyst mixture. The research on bifunctional materials is still in its infancy, but the inherent improvement in kinetics and stability, compared to hybrid-type materials, brings forth alkali metal ceramics Li_2ZrO_3, Li_4SiO_4 and Na_2ZrO_3 as bifunctional candidates. Their possible applications in this regard have not been explored as yet in our knowledge. Alkali metal ceramics have been investigated as CO_2 sorbents in the context of post-combustion scenarios i.e. CO_2 capture from flue gas. These sorbents have been extensively studied over past 15 years showing an improved performance as their chemisorption mechanism is understood and refinements in their synthesis methods have been reported. Furthermore, alkali metal carbonates, which are formed as a result of CO_2 chemisorption by alkali metal sorbents, possess catalytic ability pyrolysis and gasification with different hydrocarbon feedstocks and solid fuels. All of this taken together clearly present a picture of a set of solid sorbents that, when utilized as bifunctional material, benefit from improved kinetics and at the same time provide the robustness under given operational conditions that are missing in CaO and HTlcs based materials.

In this context, alkali metal ceramics can be paired with conventional Ni catalyst to provide absorptive support as well as a highly durable structure. The variance in effective methods to synthesize alkali metal ceramics will be effective in controlling the morphology of the material, providing a suitable porous structure to disperse the selected catalyst upon. Likewise, the sturdiness of alkali metal ceramics eliminates the necessity

753 of using other metal refractory supports, resulting in a simplified synthesis process

754 consisting of only two materials, the catalyst and the sorbent. This is important because it

755 provides ease in manipulating the concentration profiles of catalyst and sorbent, and their

756 placements within the final material. Theoretical studies on bifunctional pellets have

757 assumed the presence of catalytic and sorbent sites within the material, their performance

758 under multi-cycle process, and the effects of variable distribution of said sites.

759 With alkali metal ceramics as bifunctional materials, it is possible to investigate the

760 validity of theoretical studies to identify the optimal makeup of a bifunctional material

761 under SESR conditions. According to the literature on catalytic abilities of alkali metal

762 carbonates, it is unlikely that a mixture of separate alkali metal zirconates/silicates and

763 carbonate phases can successfully fulfill the dual roles of catalyst and sorbent on its own.

764 However, the eventual formation of alkali metal carbonates in a bifunctional material as a

765 result of alkali metal ceramics carbonation adds an interesting dimension to their

766 potential future use in SESR. Alkali metal carbonates have been previously used as a

767 primary catalyst to breakdown larger hydrocarbon chains, and their presence as an

768 auxiliary catalyst should further increase the value of alkali metal ceramics as

769 bifunctional materials.

776

777 **REFERENCES**

778 1.　　Florin, N. H.; Harris, A. T., Enhanced hydrogen production from biomass with in

779 situ carbon dioxide capture using calcium oxide sorbents. *Chem. Eng. Sci.* **2008**, 63, 287-

780 316.

781 2.　　Sikarwar, V. S.; Zhao, M.; Clough, P.; Yao, J.; Zhong, X.; Memon, M. Z.; Shah,

782 N.; Anthony, E. J.; Fennell, P. S., An overview of advances in biomass gasification.

783 *Energ. Environ. Sci.* **2016**, 9, 2939-2977.

784 3.　　Balat, M., Potential importance of hydrogen as a future solution to environmental

785 and transportation problems. *Int. J. Hydrogen Energ.* **2008**, 33, 4013-4029.

786 4.　　Armor, J. N., The multiple roles for catalysis in the production of H_2. *Appl. Catal.*

787 *A-Gen.* **1999**, 176, 159-176.

788 5.　　Hufton, J. R.; Mayorga, S.; Sircar, S., Sorption-enhanced reaction process for

789 hydrogen production. *Aiche J.* **1999**, 45, 248-256.

790 6.　　Balasubramanian, B.; López Ortiz, A.; Kaytakoglu, S.; Harrison, D. P., Hydrogen

791 from methane in a single-step process. *Chem. Eng. Sci.* **1999**, 54, 3543-3552.

792   7.   Kato, M.; Maezawa, Y.; Takeda, S.; Hagiwara, Y.; Kogo, R.; Semba, K.;

793   Hamamura, M., Pre-combustion CO_2 capture using ceramic absorbent and methane steam

794   reforming. *Key Eng. Mat.* **2006**, 317-318, 81-84.

795   8.   Sutton, D.; Kelleher, B.; Ross, J. R. H., Review of literature on catalysts for

796   biomass gasification. *Fuel. Process. Technol.* **2001**, 73, 155-173.

797   9.   Lee, K. B.; Beaver, M. G.; Caram, H. S.; Sircar, S., Reversible chemisorbents for

798   carbon dioxide and their potential applications. *Ind. Eng. Chem. Res.* **2008**, 47, 8048-

799   8062.

800   10.   Aaron, D.; Tsouris, C., Separation of CO_2 from flue gas: A review. *Sep. Sci.*

801   *Technol.* **2005**, 40, 321-348.

802   11.   Choi, S.; Drese, J. H.; Jones, C. W., Adsorbent materials for carbon dioxide

803   capture from large anthropogenic point sources. *ChemSusChem* **2009**, 2, 796-854.

804   12.   Grasa, G. S.; Abanades, J. C., CO_2 capture capacity of CaO in long series of

805   carbonation/calcination cycles. *Ind. Eng. Chem. Res*. **2006**, 45, 8846-8851.

806   13.   Martavaltzi, C. S.; Lemonidou, A. A., Development of new CaO based sorbent

807   materials for CO_2 removal at high temperature. *Micropor. Mesopor. Mat.* **2008**, 110, 119-

808   127.

809   14.   Ding, Y.; Alpay, E., Equilibria and kinetics of CO_2 adsorption on hydrotalcite

810   adsorbent. *Chem. Eng. Sci.* **2000**, 55, 3461-3474.

811   15.   Lee, S. C.; Choi, B. Y.; Lee, T. J.; Ryu, C. K.; Ahn, Y. S.; Kim, J. C., CO_2

812   absorption and regeneration of alkali metal-based solid sorbents. *Catal. Today* **2006**, 111,

813   385-390.

814   16.   Bhatta, L. K. G.; Subramanyam, S.; Chengala, M. D.; Olivera, S.; Venkatesh, K.,

815   Progress in hydrotalcite like compounds and metal-based oxides for CO_2 capture: A

816   review. *J. Clean. Prod.* **2015**, 103, 171-196.

817   17.   Dou, B.; Wang, C.; Song, Y.; Chen, H.; Jiang, B.; Yang, M.; Xu, Y., Solid

818   sorbents for in-situ CO_2 removal during sorption-enhanced steam reforming process: A

819   review. *Renew. Sust. Energ. Rev.* **2016**, 53, 536-546.

820   18.   Lugo, E. L.; Wilhite, B. A., A theoretical comparison of multifunctional catalyst

821   for sorption-enhanced reforming process. *Chem. Eng. Sci.* **2016**, 150, 1-15.

822   19.   Dietrich, W.; Lawrence, P. S.; Grünewald, M.; Agar, D. W., Theoretical studies

823   on multifunctional catalysts with integrated adsorption sites. *Chem. Eng. J.* **2005**, 107,

824   103-111.

825   20.   Pfeiffer, H., Advances on alkaline ceramics as possible CO_2 captors. In *Advances*

826   *in CO2 Conversion and Utilization*, American Chemical Society: **2010**; Vol. 1056, pp

827   233-253.

828   21.   Alcántar-Vázquez, B.; Vera, E.; Buitron-Cabrera, F.; Lara, Garcia, H. A.; Pfeiffer,

829   H., Evidence of CO oxidation-chemisorption process on sodium zirconate (Na_2ZrO_3).

830   *Chem. Lett*. **2015**, 44, 480-482.

831   22.   Mudge, L. K.; Baker, E. G.; Mitchell, D. H.; Brown, M. D., Catalytic steam

832   gasification of biomass for methanol and methane production. *J. Sol. Energ.-T. Asme*

833   **1985**, 107, 88-92.

834   23.   Fahmi, R.; Bridgwater, A. V.; Darvell, L. I.; Jones, J. M.; Yates, N.; Thain, S.;

835   Donnison, I. S., The effect of alkali metals on combustion and pyrolysis of Lolium and

836   Festuca grasses, switchgrass and willow. *Fuel* **2007**, 86, 1560-1569.

837   24.   Santiago-Torres, N.; Romero-Ibarra, I. C.; Pfeiffer, H., Sodium zirconate

838   (Na_2ZrO_3) as a catalyst in a soybean oil transesterification reaction for biodiesel

839   production. *Fuel Process. Technol.* **2014**, 120, 34-39.

840   25.   Ochoa-Fernández, E.; Rusten, H. K.; Jakobsen, H. A.; Rønning, M.; Holmen, A.;

841   Chen, D., Sorption enhanced hydrogen production by steam methane reforming using

842   Li_2ZrO_3 as sorbent: Sorption kinetics and reactor simulation. *Catal. Today* **2005**, 106, 41-

843   46.

844   26.   Rusten, H. K.; Ochoa-Fernández, E.; Lindborg, H.; Chen, D.; Jakobsen, H. A.,

845   Hydrogen production by sorption-enhanced steam methane reforming using lithium

846   oxides as CO_2-acceptor. *Ind. Eng. Chem. Res*. **2007**, 46, 8729-8737.

847   27.   Rusten, H. K.; Ochoa-Fernandez, E.; Chen, D.; Jakobsen, H. A., Numerical

848   investigation of sorption enhanced steam methane reforming using Li_2ZrO_3 as CO_2-

849   acceptor. *Ind. Eng. Chem. Res* **2007**, 46, 4435-4443.

850   28.   Aceves Olivas, D. Y.; Baray Guerrero, M. R.; Escobedo Bretado, M. A.; Marques

851   Da Silva Paula, M.; Salinas Gutiérrez, J.; Guzmán Velderrain, V.; López Ortiz, A.;

852 Collins-Martínez, V., Enhanced ethanol steam reforming by CO_2 absorption using CaO,

853 CaO∗MgO or Na_2ZrO_3. *Int. J. Hydrogen Energ.* **2014**, 39, 16595-16607.

854 29. Harrison, D. P., Sorption-enhanced hydrogen production: A review. *Ind. Eng.*

855 *Chem. Res.* **2008**, 47, 6486-6501.

856 30. Satrio, J. A.; Shanks, B. H.; Wheelock, T. D., Development of a novel combined

857 catalyst and sorbent for hydrocarbon reforming. *Ind. Eng. Chem. Res*. **2005**, 44, 3901-

858 3911.

859 31. Dewoolkar, K. D.; Vaidya, P. D., Improved hydrogen production by sorption-

860 enhanced steam methane reforming over hydrotalcite- and calcium-based hybrid

861 materials. *Energ. Fuel.* **2015**, 29, 3870-3878.

862 32. Martavaltzi, C. S.; Lemonidou, A. A., Hydrogen production via sorption

863 enhanced reforming of methane: Development of a novel hybrid material—reforming

864 catalyst and CO_2 sorbent. *Chem. Eng. Sci.* **2010**, 65, 4134-4140.

865 33. Chanburanasiri, N.; Ribeiro, A. M.; Rodrigues, A. E.; Arpornwichanop, A.;

866 Laosiripojana, N.; Praserthdam, P.; Assabumrungrat, S., Hydrogen production via

867 sorption enhanced steam methane reforming process using Ni/CaO multifunctional

868 catalyst. *Ind. Eng. Chem. Res.* **2011**, 50, 13662-13671.

869 34. Nahil, M. A.; Wang, X.; Wu, C.; Yang, H.; Chen, H.; Williams, P. T., Novel bi-

870 functional Ni-Mg-Al-CaO catalyst for catalytic gasification of biomass for hydrogen

871 production with in situ CO_2 adsorption. *RSC Adv.* **2013**, 3, 5583-5590.

872   35.   Radfarnia, H. R.; Iliuta, M. C., Development of Al-stabilized CaO–nickel hybrid

873   sorbent–catalyst for sorption-enhanced steam methane reforming. *Chem. Eng. Sci.* **2014**,

874   109, 212-219.

875   36.   Radfarnia, H. R.; Iliuta, M. C., Hydrogen production by sorption-enhanced steam

876   methane reforming process using CaO-Zr/Ni bifunctional sorbent–catalyst. *Chem. Eng.*

877   *Process*. **2014**, 86, 96-103.

878   37.   Ashok, J.; Kathiraser, Y.; Ang, M. L.; Kawi, S., Bi-functional hydrotalcite-

879   derived $NiO–CaO–Al_2O_3$ catalysts for steam reforming of biomass and/or tar model

880   compound at low steam-to-carbon conditions. *Appl. Catal. B-Environ.* **2015**, 172–173,

881   116-128.

882   38.   Xu, P.; Zhou, Z.; Zhao, C.; Cheng, Z., Catalytic performance of Ni/CaO-

883    $Ca_5Al_6O_{14}$ bifunctional catalyst extrudate in sorption-enhanced steam methane reforming.

884   *Catal. Today* **2016**, 259, 347-353.

885   39.   Wu, G.; Zhang, C.; Li, S.; Huang, Z.; Yan, S.; Wang, S.; Ma, X.; Gong, J.,

886   Sorption enhanced steam reforming of ethanol on $Ni-CaO-Al_2O_3$ multifunctional

887   catalysts derived from hydrotalcite-like compounds. *Energ. Environ. Sci.* **2012**, 5, 8942-

888   8949.

889   40.   Kong, M.; Albrecht, K. O.; Shanks, B. H.; Wheelock, T. D., Development of a

890   combined catalyst and sorbent for the water gas shift reaction. *Ind. Eng. Chem. Res*.

891   **2014**, 53, 9570-9577.

49

892   41.   Broda, M.; Kierzkowska, A. M.; Baudouin, D.; Imtiaz, Q.; Copéret, C.; Müller, C.

893   R., Sorbent-enhanced methane reforming over a Ni–Ca-based, bifunctional catalyst

894   sorbent. *ACS Catal.* **2012**, 2, 1635-1646.

895   42.   Dewoolkar, K. D.; Vaidya, P. D., Tailored hydrotalcite-based hybrid materials for

896   hydrogen production via sorption-enhanced steam reforming of ethanol. *Int. J. Hydrogen*

897   *Energ.* **2016**, 41, 6094-6106.

898   43.   Cunha, A. F.; Wu, Y.-J.; Li, P.; Yu, J.-G.; Rodrigues, A. E., Sorption-enhanced

899   steam reforming of ethanol on a novel K–Ni–Cu–hydrotalcite hybrid material. *Ind. Eng.*

900   *Chem. Res.* **2014**, 53, 3842-3853.

901   44.   Wu, Y. J.; Li, P.; Yu, J. G.; Cunha, A. F.; Rodrigues, A. E., Sorption-enhanced

902   steam reforming of ethanol on NiMgAl multifunctional materials: Experimental and

903   numerical investigation. *Chem. Eng. J.* **2013**, 231, 36-48.

904   45.   Cunha, A. F.; Wu, Y. J.; Santos, J. C.; Rodrigues, A. E., Sorption enhanced steam

905   reforming of ethanol on hydrotalcite-like compounds impregnated with active copper.

906   *Chem. Eng. Res. Des.* **2013**, 91, 581-592.

907   46.   Nakagawa, K.; Ohashi, T., A novel method of CO_2 capture from high temperature

908   gases. *J. Electrochem. Soc.* **1998**, 145, 1344-1346.

909   47.   Nakagawa, K.; Ohashi, T., A reversible change between lithium zirconate and

910   zirconia in molten carbonate. *Electrochemistry* **1999**, 67, 618-621.

911 48. Nair, B. N.; Yamaguchi, T.; Kawamura, H.; Nakao, S.-I.; Nakagawa, K.,

912 Processing of lithium zirconate for applications in carbon dioxide separation: Structure

913 and properties of the powders. *J. Am. Ceram. Soc.* **2004**, 87, 68-74.

914 49. Nair, B. N.; Burwood, R. P.; Goh, V. J.; Nakagawa, K.; Yamaguchi, T., Lithium

915 based ceramic materials and membranes for high temperature CO_2 separation. *Prog.*

916 *Mater. Sci.* **2009**, 54, 511-541.

917 50. Zhao, T.; Ochoa-Fernández, E.; Rønning, M.; Chen, D., Preparation and high-

918 temperature CO_2 capture properties of nanocrystalline Na_2ZrO_3. *Chem. Mater.* **2007**, 19,

919 3294-3301.

920 51. Alcérreca-Corte, I.; Fregoso-Israel, E.; Pfeiffer, H., CO_2 absorption on Na_2ZrO_3:

921 A kinetic analysis of the chemisorption and diffusion processes. *J. Phys. Chem. C* **2008**,

922 112, 6520-6525.

923 52. Santillán-Reyes, G. G.; Pfeiffer, H., Analysis of the CO_2 capture in sodium

924 zirconate (Na_2ZrO_3). Effect of the water vapor addition. *Int. J. Greenh. Gas Con.* **2011**, 5,

925 1624-1629.

926 53. Martínez-dlCruz, L.; Pfeiffer, H., Microstructural thermal evolution of the

927 Na_2CO_3 phase produced during a Na_2ZrO_3–CO_2 chemisorption process. *J. Phys. Chem. C*

928 **2012**, 116, 9675-9680.

929 54. Martínez-dlCruz, L.; Pfeiffer, H., Cyclic CO_2 chemisorption–desorption behavior

930 of Na_2ZrO_3: Structural, microstructural and kinetic variations produced as a function of

931 temperature. *J. Solid State Chem.* **2013**, 204, 298-304.

51

932 55. Duan, Y., A first-principles density functional theory study of the electronic

933 structural and thermodynamic properties of M_2ZrO_3 and M_2CO_3 (M = Na, K) and their

934 capabilities for CO_2 capture. *J. Renew. Sustain. Ener.* **2012**, 4, 013109.

935 56. Wyers, G. P.; Cordfunke, E. H. P., Phase relations in the system Li_2O-ZrO_2. *J.*

936 *Nucl. Mater.* **1989**, 168, 24-30.

937 57. Yin, X.-S.; Li, S.-P.; Zhang, Q.-H.; Yu, J.-G., Synthesis and CO_2 adsorption

938 characteristics of lithium zirconates with high lithia content. *J. Am. Ceram. Soc.* **2010**, 93,

939 2837-2842.

940 58. Guo, L.; Wang, X.; Zhong, C.; Li, L., Synthesis and CO_2 capture property of high

941 aspect-ratio Li_2ZrO_3 nanotubes arrays. *Appl. Surf. Sci*. **2011**, 257, 8106-8109.

942 59. Yin, X.-S.; Zhang, Q.-H.; Yu, J.-G., Three-step calcination synthesis of high-

943 purity Li_8ZrO_6 with CO_2 absorption properties. *Inorg. Chem*. **2011**, 50, 2844-2850.

944 60. Ida, J.; Lin, Y. S., Mechanism of high-temperature CO_2 sorption on lithium

945 zirconate. *Environ. Sci. Technol*. **2003**, 37, 1999-2004.

946 61. Kato, M.; Yoshikawa, S.; Nakagawa, K., Carbon dioxide absorption by lithium

947 orthosilicate in a wide range of temperature and carbon dioxide concentrations. *J. Mater,*

948 *Sci. Lett*. **2002**, 21, 485-487.

949 62. Duan, Y.; Parlinski, K., Density functional theory study of the structural,

950 electronic, lattice dynamical, and thermodynamic properties of Li_4SiO_4 and its capability

951 for CO_2 capture. *Phys. Rev. B* **2011**, 84, 104113.

952 63.   Pacciani, R.; Torres, J.; Solsona, P.; Coe, C.; Quinn, R.; Hufton, J.; Golden, T.;

953 Vega, L. F., Influence of the concentration of CO_2 and SO_2 on the absorption of CO_2 by a

954 lithium orthosilicate-based absorbent. *Environ. Sci. Technol*. **2011**, 45, 7083-7088.

955 64.   Duran-Munoz, F.; Romero-Ibarra, I. C.; Pfeiffer, H., Analysis of the CO_2

956 chemisorption reaction mechanism in lithium oxosilicate (Li_8SiO_6): A new option for

957 high-temperature CO_2 capture. *J. Mater. Chem. A* **2013**, 1, 3919-3925.

958 65.   Duan, Y.; Pfeiffer, H.; Li, B.; Romero-Ibarra, I. C.; Sorescu, D. C.; Luebke, D.

959 R.; Halley, J. W., CO_2 capture properties of lithium silicates with different ratios of

960 Li_2O/SiO_2: An ab initio thermodynamic and experimental approach. *Phys. Chem. Chem.*

961 *Phys*. **2013**, 15, 13538-13558.

962 66.   Kato, M.; Nakagawa, K., New series of lithium containing complex oxides,

963 lithium silicates, for application as a high temperature CO_2 absorbent. *J. Ceram. Soc. Jpn.*

964 **2001**, 109, 911-914.

965 67.   Rodríguez, M. T.; Pfeiffer, H., Sodium metasilicate (Na_2SiO_3): A thermo-kinetic

966 analysis of its CO_2 chemical sorption. *Thermochim. Acta* **2008**, 473, 92-95.

967 68.   Ávalos-Rendón, T.; Lara, V. H.; Pfeiffer, H., CO_2 chemisorption and cyclability

968 analyses of lithium aluminate polymorphs (α- and β- Li_5AlO_4). *Ind. Eng. Chem. Res*.

969 **2012**, 51, 2622-2630.

970 69.   Palacios-Romero, L. M.; Pfeiffer, H., Lithium cuprate (Li_2CuO_2): A new possible

971 ceramic material for CO_2 chemisorption. *Chem. Lett*. **2008**, 37, 862-863.

972 70. Oh-ishi, K.; Matsukura, Y.; Okumura, T.; Matsunaga, Y.; Kobayashi, R.,

973 Fundamental research on gas–solid reaction between CO_2 and Li_2CuO_2 linking

974 application for solid CO_2 absorbent. *J. Solid State Chem*. **2014**, 211, 162-169.

975 71. Togashi, N.; Okumura, T.; Oh-Ishi, K., Synthesis and CO_2 absorption property of

976 Li_4TiO_4 as a novel CO_2 absorbent. *J. Ceram. Soc. Jpn.* **2007**, 115, 324-328.

977 72. Sánchez-Camacho, P.; Romero-Ibarra, I. C.; Duan, Y.; Pfeiffer, H.,

978 Thermodynamic and kinetic analyses of the CO_2 chemisorption mechanism on Na_2TiO_3:

979 Experimental and theoretical evidences. *J. Phys. Chem. C* **2014**, 118, 19822-19832.

980 73. Kato, M.; Essaki, K.; Nakagawa, K.; Suyama, Y.; Terasaka, K., CO_2 absorption

981 properties of lithium ferrite for application as a high-temperature CO_2 absorbent. *J Ceram

982 Soc. Jpn.* **2005**, 113, 684-686.

983 74. Ochoa-Fernández, E.; Rønning, M.; Grande, T.; Chen, D., Synthesis and CO_2

984 capture properties of nanocrystalline lithium zirconate. *Chem. Mater*. **2006**, 18, 6037-

985 6046.

986 75. Ochoa-Fernández, E.; Rønning, M.; Grande, T.; Chen, D., Nanocrystalline lithium

987 zirconate with improved kinetics for high-temperature CO_2 capture. *Chem. Mater*. **2006**,

988 18, 1383-1385.

989 76. Xiao, Q.; Liu, Y.; Zhong, Y.; Zhu, W., A citrate sol-gel method to synthesize

990 Li_2ZrO_3 nanocrystals with improved CO_2 capture properties. *J. Mater. Chem*. **2011**, 21,

991 3838-3842.

992 77.   Iwan, A.; Stephenson, H.; Ketchie, W. C.; Lapkin, A. A., High temperature

993 sequestration of CO_2 using lithium zirconates. *Chem. Eng. J.* **2009**, 146, 249-258.

994 78.   Radfarnia, H. R.; Iliuta, M. C., Surfactant-template/ultrasound-assisted method

995 for the preparation of porous nanoparticle lithium zirconate. *Ind. Eng. Chem. Res*. **2011**,

996 50, 9295-9305.

997 79.   Kang, S.-Z.; Wu, T.; Li, X.; Mu, J., Low temperature biomimetic synthesis of the

998 Li_2ZrO_3 nanoparticles containing $Li_6Zr_2O_7$ and high temperature CO_2 capture. *Mater.*

999 *Lett*. **2010**, 64, 1404-1406.

1000 80.   Khokhani, M.; Khomane, R. B.; Kulkarni, B. D., Sodium-doped lithium zirconate

1001 nano squares: Synthesis, characterization and applications for CO_2 sequestration. *J. Sol-*

1002 *Gel Sci. Techn.* **2012**, 61, 316-320.

1003 81.   Guo, L.; Wang, X.; Zhang, S.; Zhong, C.; Li, L., Effect of alkalinity on the

1004 hydrothermal synthesis of Li_2ZrO_3 nanotube arrays. *J. Mater. Sci.* **2011**, 46, 6960-6963.

1005 82.   Yi, K. B.; Eriksen, D. Ø., Low temperature liquid state synthesis of lithium

1006 zirconate and its characteristics as a CO_2 sorbent. *Sep. Sci. Technol.* **2006**, 41, 283-296.

1007 83.   Halabi, M. H.; de Croon, M. H. J. M.; van der Schaaf, J.; Cobden, P. D.;

1008 Schouten, J. C., Reactor modeling of sorption-enhanced autothermal reforming of

1009 methane. Part I: Performance study of hydrotalcite and lithium zirconate-based processes.

1010 *Chem. Eng. J.* **2011**, 168, 872-882.

1011 84.   Essaki, K.; Nakagawa, K.; Kato, M.; Uemoto, H., CO_2 absorption by lithium

1012 silicate at room temperature. *J. Chem. Eng. Jpn*. **2004**, 37, 772-777.

1013   85.   Venegas, M. J.; Fregoso-Israel, E.; Escamilla, R.; Pfeiffer, H., Kinetic and

1014   reaction mechanism of CO_2 sorption on Li_4SiO_4: Study of the particle size effect. *Ind.*

1015   *Eng. Chem. Res*. **2007**, 46, 2407-2412.

1016   86.   Wang, K.; Guo, X.; Zhao, P.; Wang, F.; Zheng, C., High temperature capture of

1017 CO_2 on lithium-based sorbents from rice husk ash. *J. Hazard. Mater.* **2011**, 189, 301-7.

1018   87.   Romero-Ibarra, I. C.; Ortiz-Landeros, J.; Pfeiffer, H., Microstructural and CO_2

1019   chemisorption analyses of Li_4SiO_4: Effect of surface modification by the ball milling

1020   process. *Thermochim. Acta* **2013**, 567, 118-124.

1021   88.   Wu, X.; Wen, Z.; Xu, X.; Wang, X.; Lin, J., Synthesis and characterization of

1022 Li_4SiO_4 nano-powders by a water-based sol–gel process. *J. Nucl. Mater*. **2009**, 392, 471-

1023   475.

1024   89.   Bretado, M. E.; Guzmán Velderrain, V.; Lardizábal Gutiérrez, D.; Collins-

1025   Martínez, V.; Ortiz, A. L., A new synthesis route to Li_4SiO_4 as CO_2 catalytic/sorbent.

1026   *Catal. Today* **2005**, 107–108, 863-867.

1027   90.   Shan, S.; Jia, Q.; Jiang, L.; Li, Q.; Wang, Y.; Peng, J., Novel Li_4SiO_4-based

1028   sorbents from diatomite for high temperature CO_2 capture. *Ceram. Int*. **2013**, 39, 5437-

1029   5441.

1030   91.   Shan, S.; Jia, Q.; Jiang, L.; Li, Q.; Wang, Y.; Peng, J., Preparation and kinetic

1031   analysis of Li_4SiO_4 sorbents with different silicon sources for high temperature CO_2

1032   capture. *Chinese Sci. Bull*. **2012**, 57, 2475-2479.

1033   92.   Olivares-Marin, M.; Drage, T. C.; Maroto-Valer, M. M., Novel lithium-based

1034   sorbents from fly ashes for CO_2 capture at high temperatures. *Int. J. Greenhouse Gas*

1035   *Control* **2010**, 4, 623-629.

1036   93.   Wang, K.; Zhao, P.; Guo, X.; Li, Y.; Han, D.; Chao, Y., Enhancement of

1037   reactivity in Li_4SiO_4-based sorbents from the nano-sized rice husk ash for high-

1038   temperature CO_2 capture. *Energy Convers. Manage*. **2014**, 81, 447-454.

1039   94.   Yang, X.; Liu, W.; Sun, J.; Hu, Y.; Wang, W.; Chen, H.; Zhang, Y.; Li, X.; Xu,

1040   M., Preparation of novel Li_4SiO_4 sorbents with superior performance at low CO_2

1041   concentration. *ChemSusChem* **2016**, 9, 1607-1613.

1042   95.   Wang, K.; Yin, Z.; Zhao, P., Synthesis of macroporous Li_4SiO_4 via a citric acid-

1043   based sol–gel route coupled with carbon coating and its CO_2 chemisorption properties.

1044   *Ceram. Int.* **2016**, 42, 2990-2999.

1045   96.   Wang, K.; Zhou, Z.; Zhao, P.; Yin, Z.; Su, Z.; Sun, J., Synthesis of a highly

1046   efficient Li_4SiO_4 ceramic modified with a gluconic acid-based carbon coating for high-

1047   temperature CO_2 capture. *Appl. Energ.* **2016**, 183, 1418-1427.

1048   97.   López‐Ortiz, A.; Rivera, N. G. P.; Rojas, A. R.; Gutierrez, D. L., Novel carbon

1049   dioxide solid acceptors using sodium containing oxides. *Sep. Sci. Technol.* **2005**, 39,

1050   3559-3572.

1051   98.   Alcántar-Vázquez, B.; Diaz, C.; Romero-Ibarra, I. C.; Lima, E.; Pfeiffer, H.,

1052   Structural and CO_2 chemisorption analyses on $Na_2(Zr_{1-x}Al_x)O_3$ solid solutions. *J. Phys.*

1053   *Chem. C* **2013**, 117, 16483-16491.

1054   99.   Ooi, K. M.; Chai, S. P.; Mohamed, A. R.; Mohammadi, M., Effects of sodium

1055   precursors and gelling agents on CO_2 sorption performance of sodium zirconate. *Asia*

1056   *Pac. J. Chem. Eng*. **2015**, *10*, 565-579.

1057   100.   Zhao, T. J.; Rønning, M.; Chen, D., Preparation of nanocrystalline Na_2ZrO_3 for

1058   high-temperature CO_2 acceptors: Chemistry and mechanism. *J. Energy Chem*. **2013**, *22*,

1059   387-393.

1060   101.   Martínez-dlCruz, L.; Pfeiffer, H., Toward understanding the effect of water

1061   sorption on lithium zirconate (Li_2ZrO_3) during its carbonation process at low

1062   temperatures. *J. Phys. Chem. C* **2010**, *114*, 9453-9458.

1063   102.   Ochoa-Fernández, E.; Rønning, M.; Yu, X.; Grande, T.; Chen, D., Compositional

1064   effects of nanocrystalline lithium zirconate on its CO_2 capture properties. *Ind. Eng.*

1065   *Chem. Res*. **2008**, *47*, 434-442.

1066   103.   Sanchez-Camacho, P.; Romero-Ibarra, I. C.; Pfeiffer, H., Thermokinetic and

1067   microstructural analyses of the CO_2 chemisorption on K_2CO_3-Na_2ZrO_3. *J. CO2 Util.*

1068   **2013**, *3-4*, 14-20.

1069   104.   Lara-Garcia, H.; Alcántar-Vázquez, B.; Duan, Y.; Pfeiffer, H., CO chemical

1070   capture on lithium cuprate, through a consecutive CO oxidation and chemisorption

1071   bifunctional process. *J. Phys. Chem. C* **2016**, *120*, 3798-3806.

1072   105.   Vera, E.; Alcántar-Vázquez, B.; Pfeiffer, H., CO_2 chemisorption and evidence of

1073   the CO oxidation–chemisorption mechanisms on sodium cobaltate. *Chem. Eng. J*. **2015**,

1074   *271*, 106-113.

1075   106.   Alcántar-Vázquez, B.; Duan, Y.; Pfeiffer, H., CO oxidation and subsequent CO_2

1076   chemisorption on alkaline zirconates: Li_2ZrO_3 and Na_2ZrO_3. *Ind. Eng. Chem. Res*. **2016**,

1077   55, 9880-9886.

1078   107.   Mendoza-Nieto, J. A.; Vera, E.; Pfeiffer, H., Methane reforming process by

1079   means of a carbonated Na_2ZrO_3 catalyst. *Chem. Lett*. **2016**, 45, 685-687.

1080   108.   Kapteijn, F.; Abbel, G.; Moulijn, J. A., CO_2 gasification of carbon catalysed by

1081   alkali metals. *Fuel* **1984**, 63, 1036-1042.

1082   109.   Karimi, A.; Gray, M. R., Effectiveness and mobility of catalysts for gasification

1083   of bitumen coke. *Fuel* **2011**, 90, 120-125.

1084   110.   Spiro, C. L.; McKee, D. W.; Kosky, P. G.; Lamby, E. J.; Maylotte, D. H.,

1085   Significant parameters in the catalysed CO_2 gasification of coal chars. *Fuel* **1983**, 62,

1086   323-330.

1087   111.   McKee, D. W.; Chatterji, D., The catalyzed reaction of graphite with water vapor.

1088   *Carbon* **1978**, 16, 53-57.

1089   112.   Yeboah, Y. D.; Xu, Y.; Sheth, A.; Godavarty, A.; Agrawal, P. K., Catalytic

1090   gasification of coal using eutectic salts: identification of eutectics. *Carbon* **2003**, 41, 203-

1091   214.

1092   113.   McKee, D. W.; Spiro, C. L.; Kosky, P. G.; Lamby, E. J., Eutectic salt catalysts for

1093   graphite and coal char gasification. *Fuel* **1985**, 64, 805-809.

1094   114.   Smets, K.; Roukaerts, A.; Czech, J.; Reggers, G.; Schreurs, S.; Carleer, R.;

1095   Yperman, J., Slow catalytic pyrolysis of rapeseed cake: Product yield and

1096   characterization of the pyrolysis liquid. *Biomass. Bioenerg.* **2013**, 57, 180-190.

1097   115.   Ramsurn, H.; Kumar, S.; Gupta, R. B., Enhancement of biochar gasification in

1098   alkali hydrothermal medium by passivation of inorganic components using $Ca(OH)_2$.

1099   *Energ. Fuel*. **2011**, 25, 2389-2398.

1100   116.   Hauserman, W. B., High-yield hydrogen production by catalytic gasification of

1101   coal or biomass. *Int. J. Hydrogen Energ.* **1994**, 19, 413-419.

1102   117.   Encinar, J. M.; Beltrán, F. J.; Ramiro, A.; González, J. F., Pyrolysis/gasification

1103   of agricultural residues by carbon dioxide in the presence of different additives: Influence

1104   of variables. *Fuel Process. Technol*. **1998**, 55, 219-233.

1105   118.   Sada, E.; Kumazawa, H.; Kudsy, M., Pyrolysis of lignins in molten salt media.

1106   *Ind. Eng. Chem. Res*. **1992**, 31, 612-616

1107   119.   Ortiz-Landeros, J.; Ávalos-Rendón, T.; Gómez-Yáñez, C.; Pfeiffer, H., Analysis

1108   and perspectives concerning CO_2 chemisorption on lithium ceramics using thermal

1109   analysis. *J Therm. Anal. Calorim.* **2012**, 108, 647-655.

1110   120.   Qi, Z.; Daying, H.; Yang, L.; Qian, Y.; Zibin, Z., Analysis of CO_2

1111   sorption/desorption kinetic behaviors and reaction mechanisms on Li_4SiO_4. *AIChE J.*

1112   **2013**, 59, 901-911.

1113   121.   Gauer, C.; Heschel, W., Doped lithium orthosilicate for absorption of carbon

1114   dioxide. *J. Mater. Sci*. **2006**, 41, 2405-2409.

1115   122.   Pfeiffer, H.; Vazquez, C.; Lara, V. H.; Bosch, P., Thermal behavior and CO_2

1116   absorption of $Li_{2-x}Na_xZrO_3$ solid solutions. *Chem. Mater*. **2007**, 19, 922-926.

1117   123.   Xiao, Q.; Tang, X.; Liu, Y.; Zhong, Y.; Zhu, W., Citrate route to prepare K-doped

1118 Li_2ZrO_3 sorbents with excellent CO_2 capture properties. *Chem. Eng. J*. **2011**, 174, 231-

1119   235.

1120   124.   Kato, M.; Nakagawa, K.; Essaki, K.; Maezawa, Y.; Takeda, S.; Kogo, R.;

1121   Hagiwara, Y., Novel CO_2 absorbents using lithium-containing oxide. *Int. J. Appl. Ceram.*

1122   *Tec.* **2005**, 2, 467-475.

1123   125.   Ochoa-Fernández, E.; Zhao, T.; Rønning, M.; Chen, D., Effects of steam addition

1124   on the properties of high temperature ceramic CO_2 acceptors. *J. Environ. Eng*. **2009**, 135,

1125   397-403.

1126   126.   Olivares-Marín, M.; Castro-Díaz, M.; Drage, T. C.; Mercedes Maroto-Valer, M.,

1127   Use of small-amplitude oscillatory shear rheometry to study the flow properties of pure

1128   and potassium-doped Li_2ZrO_3 sorbents during the sorption of CO_2 at high temperatures.

1129   *Sep. Purif. Technol.* **2010**, 73, z415-420.

1130   127.   Fauth, D. J.; Frommell, E. A.; Hoffman, J. S.; Reasbeck, R. P.; Pennline, H. W.,

1131   Eutectic salt promoted lithium zirconate: Novel high temperature sorbent for CO_2

1132   capture. *Fuel Process. Technol*. **2005**, 86, 1503-1521.

1133   128.   Wang, S.; An, C.; Zhang, Q.-H., Syntheses and structures of lithium zirconates for

1134   high-temperature CO_2 absorption. *J. Mater. Chem. A* **2013**, 1, 3540-3550.

1135   129.   Seggiani, M.; Puccini, M.; Vitolo, S., Alkali promoted lithium orthosilicate for

1136 CO_2 capture at high temperature and low concentration. *Int. J. Greenhouse Gas Control*

1137   **2013**, 17, 25-31.

1138   130.   Duan, Y.; Lekse, J.; Wang, X.; Li, B.; Alcántar-Vázquez, B.; Pfeiffer, H.; Halley,

1139   J. W., Electronic structure, phonon dynamical properties, and CO_2 capture capability of

1140 $Na_{2-x}M_xZrO_3$ (M=Li, K): Density-functional calculations and experimental validations.

1141   *Phys. Rev. Appl.* **2015**, 3, 044013.

1142